CIRCULAR EDGE BOW-TIE NANO-ANTENNA FOR ENERGY HARVESTING SYSTEMS

AHASANUL HAQUE

DEPARTMENT OF ELECTRICAL ENGINEERING
FACULTY OF ENGINEERING
UNIVERSITY OF MALAYA
KUALA LUMPUR

2016

CIRCULAR EDGE BOW-TIE NANO-ANTENNA FOR ENERGY HARVESTING SYSTEMS

AHASANUL HAQUE

DISSERTATION SUBMITTED IN FULFILMENT OF THE REQUIREMENTS FOR THE DEGREE OF MASTER OF ENGINEERING SCIENCE

DEPARTMENT OF ELECTRICAL ENGINEERING

FACULTYOF ENGINEERING

UNIVERSITY OF MALAYA

KUALA LUMPUR

2016

UNIVERSITY OF MALAYA

ORIGINAL LITERARY WORK DECLARATION

Name of Candidate: Ahasanul Haque

Registration/Matric No: **KGA130056**

Name of Degree: Master of Engineering Science

Title of Project Paper/ Research Report/ Dissertation/ Thesis ("This Work"):

Circular edge bow-tie nano-antenna for energy harvesting systems

Field of Study: Renewable Energy

I do solemnly and sincerely declare that:

(1) I am the sole author/writer of this Work;
(2) This work is original;
(3) Any use of any work in which copyright exists was done by way of fair dealing and for permitted purpose and any excerpt from, or reference to or reproduction of any copyright work has been disclose expressly and sufficiently and the title of the Work and its authorship have been acknowledge in this Work;
(4) I do not have any actual knowledge nor do I ought reasonably to know that the making of this work constitutes an infringement of any copyright work;
(5) I hereby assign all and every rights in the copyright to this work to the University of Malaya (UM), who henceforth shall be owner of the copyright in this work and that any written consent of UM having been first had and obtained;
(6) I am fully aware that if in the course of making this work I have infringed any copyright whether intentionally or otherwise, I am be subject to legal action or any other action as may be determined by UM.

Candidate's Signature Date

Subscribed and solemnly declared before,

Witness's Signature Date

Name:

Designation:

ABSTRACT

In recent years, a remarkable progress has been observed in the field of energy harvesting via nano-antenna which seems to be a prominent alternative of fossil fuels as this energy is converted from tera hertz range of infrared region. In this study, a novel nano-antenna is designed in order to convert the high frequency solar energy, thermal energy or earth re-emitted sun's energy into electricity. The proposed antenna is gold printed on a SiO_2 layer, designed as a circular edge bow-tie with a ground plane at the bottom of the substrate. The Lorentz-Drude model is used to analyse the behaviour of gold at the infrared band of frequencies. The proposed antenna is designed by 3D-electromagnetic solver, and analysed for optimization of metal thickness, gap size, and antenna's geometrical length. Simulations are conducted in order to investigate the behaviour of the antenna illuminated by the circularly polarized plane wave. Also, numerical simulations are studied for improving the harvesting E-field of the antenna within 5 THz - 40 THz frequency range and performance is evaluated with respect to different slots in structural geometry. The proposed antenna offers multiple resonance frequency and better return loss within the frequency bands of 23.2 THz to 27 THz (bandwidth 3.8 THz) and 31 THz to 35.9 THz (bandwidth 4.9 THz). An output electric field of 0.656 V/μm is simulated at 25.3 THz. The best fitted gap size at the feed point is achieved as 50 nm with the substrate thickness of 1.2 μm. This study has forecasted its application in next generation solar energy harvesting round the clock for getting higher efficiency, better performance and prolonged operational life.

ABSTRAK

Dalam tahun kebelakangan ini, kemajuan yang luar biasa telah diperhatikan di dalam bidang penuaian tenaga melalui antena nano yang seolah-olah menjadi alternatif yang terkemuka untuk bahan api fosil sebagai tenaga ditukar dari jarak rantau terahertz ke rantau inframerah. Dalam kajian ini, antena nano yang baru direka untuk menukarkan frekuensi tinggi tenaga solar, tenaga haba atau tenaga matahari yang dipancarkan semula ke bumi untuk menjadi tenaga elektrik. Antena yang dicadangkan adalah emas yang dicetak pada lapisan SiO2, direka sebagai sisi bulat dan ikatan bow dengan satah rata di bahagian bawah substrat. Model Lorentz-Drude digunakan untuk menganalisis kelakuan emas di band frekuensi inframerah. Antena yang dicadangkan direka oleh penyelesai 3D-elektromagnetik, dan dianalisis untuk pengoptimuman ketebalan logam, saiz jurang, dan panjang geometri antena. Simulasi dijalankan untuk menyiasat ciri-ciri antena yang diterangi oleh gelombang satah polarisasi membulat. Juga, simulasi berangka dikaji untuk meningkatkan penuaian antena medan-E dalam tempoh 5 THz - julat frekuensi 40 THz dan prestasi dinilai tentang slot yang berbeza dalam geometri struktur. Antena yang dicadangkan menawarkan frekuensi resonans berbilang dan kehilangan pulangan yang lebih baik dalam jalur frekuensi 23.2 THz kepada 27 THz (jalur lebar 3,8 THz) dan 31 THz kepada 35.9 THz (jalur lebar 4.9 THz). Medan output elektrik 0,656 V / mikron adalah disimulasikan di 25.3 THz. Saiz jurang terbaik dipasang pada ketika suapan dicapai 50 nm dengan ketebalan substrat 1.2 mikron. Kajian ini dijangkakan aplikasinya di dalam generasi akan datang untuk penuaian tenaga solar sepanjang masa dan mendapatkan kecekapan yang lebih tinggi, prestasi yang lebih baik dan kehidupan operasi yang berpanjangan.

ACKNOWLEDGEMENT

With the deepest gratitude and indebtedness, I would like to thank to my supervisors, Dr. Ahmed Wasif Reza and Dr. Narendra Kumar for providing me a definite guidelines and intellectual support. Their kind attitude, patience, sincere sympathy, encouragement and invaluable suggestions always inspired me to complete this research work steadfastly. It was completely impossible to finish this project work without their kind help. I am so much grateful to my supervisors for their great support.

I would like to acknowledge and thank the Ministry of Higher Education, Malaysia for providing the fund of this research work under HIR-MOHE project UM.C/HIR/MOHE/ENG/51.

I am also thankful and grateful to my parents for their never-ending support, love and continuous encouragement in the bad phase of my life that helped me a lot for finishing this work. I feel a profound sense of gratitude towards my wife who had been there to support me at every stage of my M.Sc. Eng. Finally, I want to appreciate everyone who has come into my life and given me inspiration through their presence.

TABLE OF CONTENTS

LIST OF FIGURES

LIST OF TABLES

LIST OF SYMBOLS

W	:	Width of the substrate
L	:	Length of the substrate
t_s	:	Thickness of the substrate
At	:	Height or thickness of the antenna
ε_r	:	Dielectric constant of substrate
λ_0	:	Free-space wavelength
λ	:	Wavelength in substrate material
λ_d	:	Dielectric wavelength
ε_{reff}	:	Effective dielectric constant of the substrate
ΔL	:	Extended length of the antenna
L_{eff}	:	Effective length of the antenna
m	:	Transverse-magnetic mode along length of the antenna
n	:	Transverse-magnetic mode along width of the antenna
c	:	Speed of light
f_0	:	Resonant frequency of the antenna
$\vec{J}_b$	:	Current density at the bottom of antenna

$\vec{J}_t$	:	Current density at the top of antenna
S_{11}	:	S-parameter
Γ	:	Reflection co-efficient
V^+	:	Amplitude of the input voltage to load
V^-	:	Amplitude of the voltage of reflected waves
Z_{in}	:	Input impedance of the antenna
Z_s	:	Impedance of the feeding network
Q	:	Quality factor
f_u	:	Upper cut-off frequency
f_l	:	Lower cut-off frequency
f_c	:	Centre frequency between lower and upper cut-off frequency
θ	:	Elevation angle of antenna's angular position
φ	:	Azimuth angle of antenna's angular position
D_1	:	Largest dimension of the antenna
P_{in}	:	Power radiated from the isotropic antenna
S	:	Density of radiated power
r	:	Radius of imaginary sphere created by spreading power

$U0$	:	Radiation intensity of the isotropic antenna
D , $D(\theta,\phi)$:		Directivity of the antenna
U	:	Radiation intensity of the antenna
$D_{\max}$	:	Maximum directivity of the antenna
$U_{\max}$	:	Maximum radiation intensity of the antenna
$G(\theta,\phi)$:		Gain of the antenna
e_{cd}	:	Radiation efficiency of the antenna
R_r	:	Radiation resistance of the antenna
R_L	:	Loss resistance of the antenna
R_{in}	:	Input resistance at the input ends of antenna
X_{in}	:	Input reactance at the input ends of antenna

LIST OF ABBREVIATIONS

RF	:	Radio Frequency
BW	:	Bandwidth
RL	:	Return Loss
TM	:	Transverse-magnetic
2G	:	Second Generation
3G	:	Third Generation
4G	:	Fourth Generation
GSM	:	Global System for Mobile Communication
PCS	:	Personal Communication System
CST	:	Computer Simulation Technology
TEM	:	Transverse-electric-magnetic
ETSI	:	European Telecommunication Standard Institute
RFID	:	Radio-frequency Identification
MIMO	:	Multiple-input Multiple-output
MOM	:	Metal Oxide Metal
MIM	:	Metal Insulator Metal
FDTD	:	Finite Difference Time Domain

HPBW : Half power beam width

VSWR : Voltage Standing Wave Ratio

CHAPTER 1: INTRODUCTION

1.1 Background

Recent years there is a remarkable progress in the field of energy harvesting via nano-antenna which is today's most challenging scientific applications to reduce the excessive use of fossil fuel. Solar cells are one of these technologies which are used to convert the sun's energy to electricity. Different types of energy harvesting system shown are in Figure 1.1 which described the process for collecting energy from different sources and converting it to electricity, and gaining interest for future energy generation source. The major limitation of photovoltaic (PV) based technologies is their low conversion efficiency. It also depended on daylight, which makes their operation sensitive to the weather conditions. Additionally, to enhance conversion efficiency, they require a mechanical sun-tracking system (Corkish, Green, & Puzzer, 2002). In order to overcome the limitation of solar PV technologies with nano-antenna, there were serious attempts in the past ten years (Berland, 2003). The major challenge in this technology is to operate the antennas at extremely short wavelength in the infrared (IR) region, i.e., very high frequencies (THz). The current progress in terahertz (THz) technology has shown a significant potential of THz radiation detection. Because of their size, the nano-antenna is capable to absorb energy in the infrared region of the spectrum. A lot of energy has been radiated by the sun, some of which absorbed by the earth and it radiate after sunset. Comparing to the solar cell efficiency, nano-antenna provide better efficiency as it can able to take in energy from both sunlight and the earth's heat. A time varying current will be induced on the antenna surface due to impinge of an electromagnetic wave to a nano-antenna, thus a voltage will be generated at the feeding point of the antenna (Bozzetti et al., 2010; Ma & Vandenbosch, 2013a). This induced current or generated voltage will oscillate at the same frequency of the incident wave.

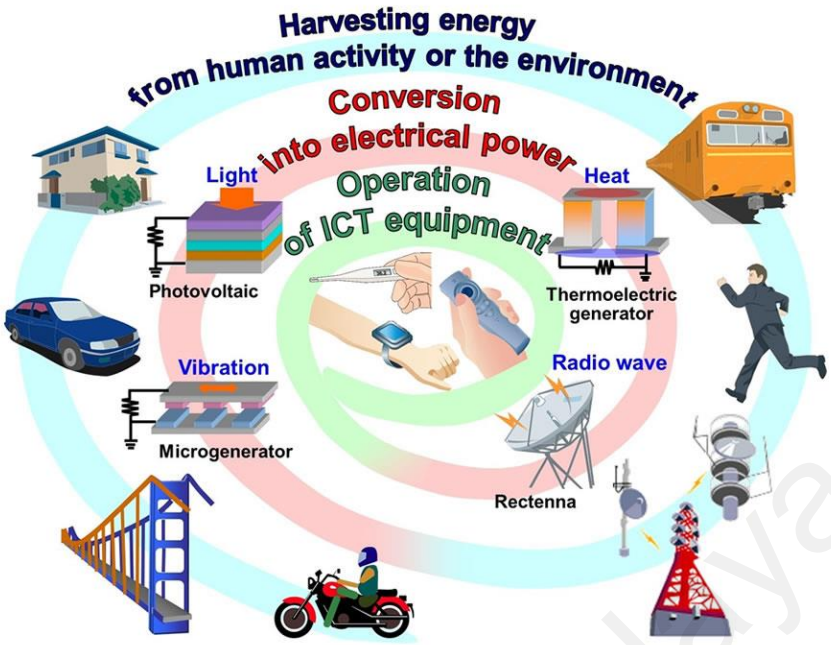

Figure 1.1: Energy harvesting from different sources (Ref: www.fujitsu.com/global/about/resources/news/press-releases/2010/1209-01.html)

In 1972, Robert Baily initially proposed nano-antenna for the energy harvesting purpose and after that many approaches and designs have been studied (Bharadwaj, Deutsch, & Novotny, 2009; Briones, Alda, & González, 2013; Kotter, Novack, Slafer, & Pinhero, 2008). The voltage or current generated in this approach will oscillate at the same frequency of the incident wave. And hence a suitable rectifier should be embedded at the feed point of the antenna in order to obtain DC power. An antenna with a rectifier circuit embedded for energy harvesting systems is called rectenna. Rectenna that consists of antennas connected to a rectifier converts the received signal to DC power and produces electricity. Wider angular reception is an important characteristic in case of antenna for energy harvesting and nano-antenna provides better angular reception characteristic comparing of PV devices. The nano-antenna does not require a sun tracking system and also does not depend on day light and hence it optimizes the solar energy collection (Berland, 2003). The total efficiency of solar harvesting system consists of two parts (Ma & Vandenbosch, 2013a; Ma, Zheng, Vandenbosch, & Moshchalkov, 2013). In the Figure

1.2 show a bow-tie shaped gold nano-antenna printed on a four layer stack up. The first layer used as an adhesion layer consist of 3 nm chromium. The second is act as matching part consist of 1.5 mm SiO_2 layer. The third layer is a 375 mm silicon reduces the substrate losses. Finally, the fourth layer is a 200 nm gold back reflector to enhance coupling to the nano-antenna from the substrate.

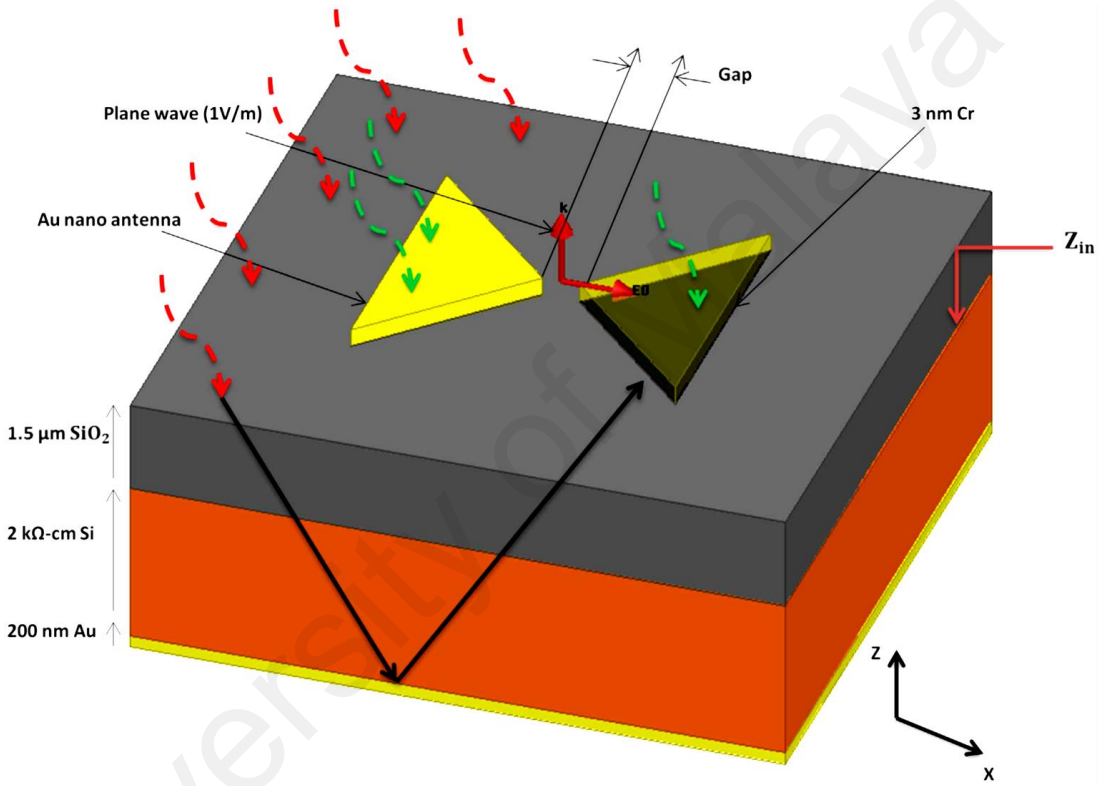

Figure 1.2: Gold nano-antenna with a substrate (Gadalla, Abdel-Rahman, & Shamim, 2014).

Figure 1.3 shows the FDTD simulation result of the field of gold nano-antenna, i.e. field intensify, current and charge distribution maps. The following Figure 1.3 shows the on-resonance near field intensity enhancement maps of the nanostructures. In Figure 1.4, it shows that nano-antenna array is used in order to increase the total energy harvesting as the single nano-antenna provides small amount of energy.

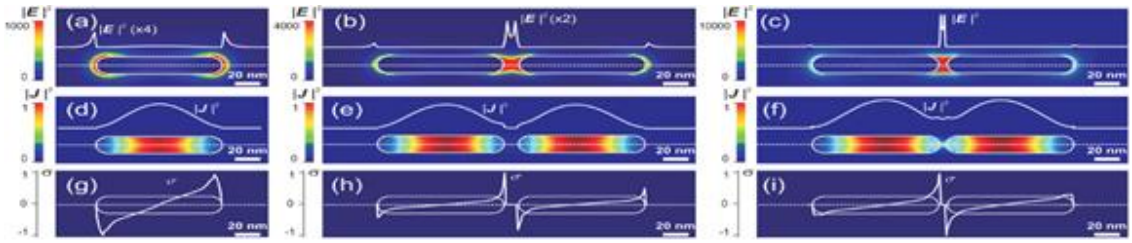

Figure 1.3: Nano-antenna for visible and infrared region. FDTD simulation result for Au nano-antenna (i) Near field intensity enhancement (a-c) (ii) Normalized current density (d-f) and (iii) Normalized surface charge densities (g-i) (Biagioni, Huang, & Hecht, 2012).

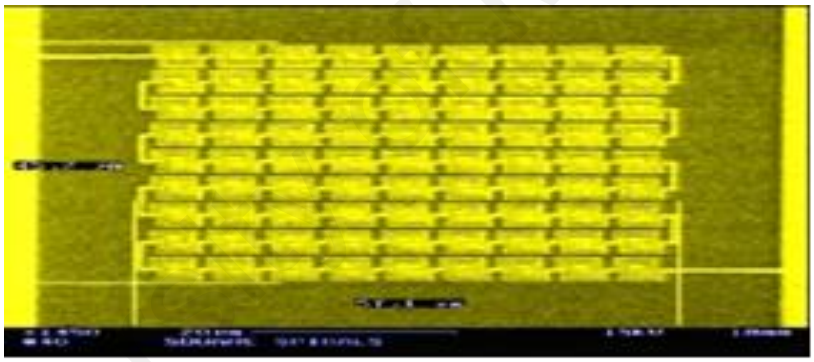

Figure 1.4: Nano-antenna array for solar energy harvesting (Biagioni et al., 2012).

1.2 Nano-antenna concept

A nano-antenna (nantenna) is a nanoscopic rectifying antenna. It is an electromagnetic collector designed to absorb specific wavelengths that are proportional to the size of the nano-antenna. Idea was first proposed by Robert L. Bailey in 1972 and received a patent in 1973 for an electromagnetic wave converter. The patented device was similar to modern day nano-antenna devices. Alvin M. Marks received a patent in 1984 for a device explicitly stating the use of sub-micron antennas for the direct conversion of light power

to electrical power. Marks's device showed substantial improvements in efficiency over Bailey's device. In 1996, Guang H. Lin was the first to report resonant light absorption by a fabricated nanostructure and rectification of light with frequencies in the visible range. Research on nano-antennas is ongoing. Nano-antennas may prove useful for converting solar radiation to electricity. Sufficient supplies of clean energy are intimately linked with global stability, economic prosperity and quality of life. Finding energy sources to satisfy the world's growing demand is one of the society's challenges for the next half century.

1.3 Problem statement

In this work, a solar energy harvesting system utilized nano-antenna is proposed. Photon energy derived from the light energy incident on the solar panel must be greater than the bandgap energy for absorbing solar radiation from the photovoltaic (PV) cell. It is required to tune the bandgap energy level with respect to the incident light energy to designing solar panel. Only 24% of light energy is absorbed by the conventional PV cell. In order to decrease solar cell expenditure and as well as to amplify the translation proficiencies, nanotechnology based techniques are prominent in nanostructure material in a solar cell (M. I. Stockman, Bergman, & Kobayashi, 2004). Another key parameter of nano-antennas in terms of optical energy harvesting is the radiation efficiency (Vandenbosch & Ma, 2012). The entire research problem can be eradicated by designing novel nano-antenna because the antenna can efficiently absorb the entire solar spectrum. There are also some research problems for designing novel nano-antenna that efficiently capture photon energy from the sun and convert it to usable power that will be used for low power devices. They are:

1. The size of the nano-antenna should be optimized for designing novel efficient solar harvesting system so that it can absorb specific wavelengths of light energy according to our desire.
2. Selection of operating frequency on which nano-antenna will operate for synchronizing with physical dimension of nano-antenna.

The main goal of this study is to design and optimize nano-antenna for capturing maximum solar and earth radiation energy.

1.4 Objectives

This research will investigate three important topics beneath a single umbrella of solar energy harvesting systems, which are listed as below:

1. Solar energy harvesting techniques
2. Nano-antenna design characteristics
3. Slotting effect in designing nano-antenna

Each and every thin film solar cell technologies have some limitations, such as: (i) indirect-bandgap semiconductor materials (like Si absorbance of near-bandgap light is little) and (ii) lack of semiconductor materials, like In and Te (Atwater & Polman, 2010). The ultimate goal of this research work is to design, investigate and simulate wideband and multiple resonance frequency nano-antenna suitable for infrared frequency range and earth re-emitted radiation to capture electromagnetic radiation for energy harvesting application.

The following two essential questions will be addressed in this research:

1. A clear identification and understanding of the incident frequency response of electromagnetic waves composed of radio waves with smaller wavelength that

will have to be received by nano-antenna and selection of the site of solar energy harvesting system.

2. A design and developing of a solar energy harvesting system using nano-antenna that will be used for capturing energy from solar energy efficiently.

Thus, this study focuses on developing novel technique for a solar energy harvesting module, improving antenna characteristics, introducing slotting effect in designing circular edge bow-tie nano-antenna for energy harvesting and modifying an energy storage system for storing harvested solar energy.

In short, the objectives of this work are:

1. To develop a novel nano-antenna used in the harvesting system for collecting solar energy.
2. To analyse slotting effect in designing a circular edge bow-tie nano-antenna for the energy harvesting system.

1.5 Organization of dissertation

The outline of this dissertation is structured as follows.

Chapter 2 describes the literature review where basic structure and operating principles of the circular edges bow-tie nano-antenna, characteristics of the bow-tie nano-antenna for terahertz (THz) application, performance parameters of nano-antenna and technical review of recent research works.

Chapter 3 presents the design procedure of the proposed antenna, simulation technique used to execute the performances of the antenna, and the method used to design the proposed antenna.

Chapter 4 explains about the simulated result obtained from proposed circular edges bowtie antenna where electric field intensity (V/μm), VSWR, surface current, current density, radiation pattern and parametric analysis are discussed in details.

Chapter 5 outlines the remarks of conclusion of this work precisely and also describes the scope of future work for this antenna.

CHAPTER 2: LITERATURE REVIEW

2.1 Introduction

The literature survey of the solar nano-antenna as a scheme for collecting solar energy mainly focuses on the following topics:

1. The antenna
2. The rectifier
3. System integration

The frame work designated for this investigation was based on the novel design and simulation with characterization and optimization of the nano-antenna.

2.2 Rectenna representation and efficiency for solar energy harvesting

The ratio of the power radiated to the power injected is known as the radiation efficiency of an antenna (Huang, Feichtner, Biagioni, & Hecht, 2009). If we consider the radiated power is P_{rad} , losses power is P_{loss} and injected power is P_{inject}, then radiation efficiency η_{rad} is given by,

$$\eta_{rad} = \frac{P_{rad}}{P_{injet}} \tag{2.1}$$

Where,

$$P_{inject} = P_{rad} + P_{loss}$$

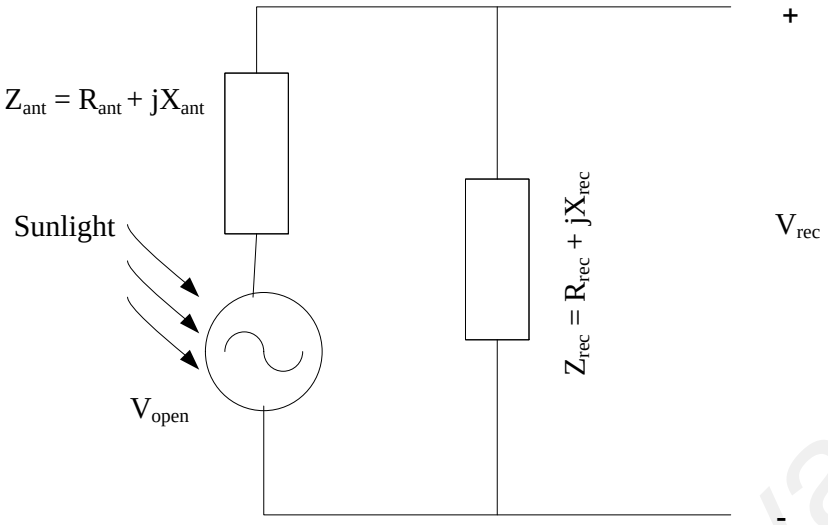

Figure 2.1: Equivalent circuit for a receiving antenna (Ma & Vandenbosch, 2013a).

Figure 2.1 shows an equivalent circuit for the receiving antenna. Here, V_{open} represents the receiving antenna generated voltage or open circuit voltage at the antenna terminals, and Z_{ant} represents the antenna impedance and Z_{rec} represents the impedance of the receiving antenna. Receiving power (P_{rec}) is given by Eqn. (2.2) (Sabaawi, Tsimenidis, & Sharif, 2013):

$$P_{rec} = \frac{R_{rec}}{2} \frac{V_{open}^2}{|Z_{ant} + Z_{rec}|\text{^}2} \tag{2.2}$$

In terms of incident electric field (E_{inj}) and the effectual length (L_{eff}), the open circuit voltage can be expressed as:

$$V_{open} = L_{eff} . E_{inj} \tag{2.3}$$

Effective length and effective area are related by the following equation:

$$L_{eff} = 2\sqrt{\frac{R_{ant}.R_{eff}}{Z_0}} \tag{2.4}$$

Where Z_0 is the intrinsic impedance of free space (Ma & Vandenbosch, 2013a).

Effective area (A_{eff}) is related to antenna gain *G* and the free space wavelength λ,

$$A_{eff} = \frac{\lambda^2.G}{4\pi} \tag{2.5}$$

Incident power (P_{inc}) density is related to the incident electric field and can be calculated by the following equation,

$$E_{inc} = \sqrt{2.Z_0.P_{inc}} \tag{2.6}$$

Combining the above Eqn. (2.3) to Eqn. (2.6) , we get,

$$V_{open} = \sqrt{\frac{2}{\pi}}.\sqrt{R_{ant}.G}.\sqrt{P_{inc}}.\lambda \tag{2.7}$$

The concluding appearance of the power established by the rectifier is given by,

$$P_{rec} = \frac{1}{\pi}.\frac{R_{rec}.R_{ant}.G.\lambda^2.P_{inc}}{|Z_{rec} + Z_{ant}|\text{^}2} = A_{ph}.P_{inc} = A_{eff}^{lossless}.P_{inc}.\eta_{mat}.\eta_{rad} \tag{2.8}$$

Where, A_{ph} = power harvesting area of the antenna.

Radiation efficiency in terms of gain and directivity is given by,

$$\eta_{rad} = \frac{G}{D} = \frac{R_{rad}}{R_{ant}} \tag{2.9}$$

The matching efficiency is given by the following equation (Ma & Vandenbosch, 2013a):

$$\eta_{rad} = \frac{4.R_{rec}.R_{ant}}{Z^2} \tag{2.10}$$

Where $Z = Z_{rec} + Z_{ant}$ total impedance. In the condition of losses free and effective area,

$$A_{eff}^{lossless} = \frac{D.\lambda^2}{4\pi} \tag{2.11}$$

From Planck's law, we know black body radiation (Ma & Vandenbosch, 2013a),

$$P_{inc}(\lambda) = \frac{2\pi hc^2}{\lambda^5} \times \frac{1}{e^{\frac{hc}{kt\lambda}-1}} \tag{2.12}$$

Where T = Surface temperature (Absolute) of the sun (in K),

h = Planck's constant (6.626×10^{-34} j),

c = Speed of light of in vacuum ($3\times10^{8} ms^{-1}$)

κ = Boltzmann constant ($1.38\times10^{-23} j$)

The following equation indicates total received power:

$$P_{total}^{rec} = \int_{\lambda_{start}}^{\lambda_{stop}} P_{rec}(\lambda).d\lambda = \int_{\lambda_{start}}^{\lambda_{stop}} \eta_{mat}(\lambda).\eta_{rad}(\lambda).A_{eff}^{lossless}(\lambda).P_{inc}(\lambda).d\lambda \tag{2.13}$$

Where λ_{start}= starting wave length of the investigated band, and λ_{stop} investigated band of the stopping wave length.

The overall efficiency (nano-antenna and rectifier) can be distinct as (Ma & Vandenbosch, 2013a),

$$\eta_{rec} = \eta_{total}^{mat}.\eta_{total}^{rad} \tag{2.14}$$

$$\eta_{total}^{rad} = \frac{\int_{\lambda_{start}}^{\lambda_{stop}} \eta_{rad}(\lambda).A_{eff}^{lossless}(\lambda).P_{inc}(\lambda).d\lambda}{\int_{\lambda_{start}}^{\lambda_{stop}} A_{eff}^{lossless}(\lambda).P_{inc}(\lambda).d\lambda} \tag{2.15}$$

$$\eta_{total}^{rad} = \frac{\int_{\lambda_{start}}^{\lambda_{stop}} \eta_{mat}(\lambda).\eta_{rad}(\lambda).A_{eff}^{lossless}(\lambda).P_{inc}(\lambda).d\lambda}{\int_{\lambda_{start}}^{\lambda_{stop}} \eta_{rad}.A_{eff}^{lossless}(\lambda).P_{inc}(\lambda).d\lambda} \tag{2.16}$$

Maximum power is impossible to be received because of the mismatch between the nano-antenna and rectifier. Antenna parameters includes as input impedance, radiation efficiency, broadside gain, lossless effective area, and effective length (Ma & Vandenbosch, 2013a).

2.3 Nano-antenna for solar energy harvesting

An inexpensive technique that collects the heat energy produced by the sun and other sources is nano-antenna. Above all, infrared radiation is an affluent energy source. To capture mid-infrared rays is primary goal of nano-antenna (Briones et al., 2013). The earth absorbs energy from the sun throughout the day and it radiates heat. Nano-antenna is a nanoscopic rectifying antenna. The nano-antenna capable to converts light and heat energy into electricity. In contrast, traditional solar cells can only use visible light. Nano-antenna or optical antenna is attractive strategies for terahertz or infrared radiation detection. Due to the fabrication of nano-antennas to form stamps of Aluminium gallium arsenide or gallium arsenide (AlGaAs/GaAs) coating, molecular beam epitaxy (MBE) method is carried out (Bareiss et al., 2011). With the intention of producing opaque arrays through electron-beam lithography technique (EBL), Si-stamps have been produced with higher number of dipole nano-antennas (more than 10 million). In order to rectify

terahertz radiation, metal-oxide metal tunnelling (MOM) diode is used which is printed with an ultrathin dielectric layer (Bareiss et al., 2011).

The main barrier for PV energy sources is the limited band gap of Si. In order to overcome the limitation of the PV solar cell as well as approaching the absorption spectrum, nano-antenna performs brilliant contenders for hybrid PV procedure which is comprising of solar cell and nano-antenna arrays (Fumeaux, Herrmann, Kneubühl, & Rothuizen, 1998; Fumeaux, Herrmann, Rothuizen, De Natale, & Kneubühl, 1996; Wilke, Oppliger, Herrmann, & Kneubühl, 1994). Due to the absorption of light in the area under 1 eV, which is correlated to the high (terahertz) frequencies corresponds to antenna length (the antenna length must be in the range of several micrometers). Terahertz signals are significant for electrical appliances due to their high-speed. To convert from high frequency AC power to the DC power is a major challenge in this field of research. The I-V characteristics of MOM diode show asymmetric response in the high frequency range (THz regime) (Bean, Tiwari, Bernstein, Fay, & Porod, 2009; Bean, Weeks, & Boreman, 2011). To fabricate single antenna configuration with incorporated MOM tunnelling diodes with excellent performance have been achieved by using EBL technique (Slovick, Bean, Krenz, & Boreman, 2010). Nano-antennas react as like as RF antennas when electromagnetic (EM) wave incident upon it. It produces AC current on the surface of the antenna at the same frequency of the incident wave. A hots spot i.e. concentrated electric field is created at the feeding point of the antenna. This concentrated electric field exploit in numerous applications, for example, photo-voltaic (PV), optical communications, near-field imaging, and sensing (Bozzetti et al., 2010; Kotter et al., 2008; Maksymov, Staude, Miroshnichenko, & Kivshar, 2012). Researcher concentrate a high efficient, less expenses rectenna system to substitute the conventional solar cells. So as to receive EM wave, the rectenna is convert the high frequency AC power to useable DC power with the

help of diode. Rectenna was first proposed by Bailey (Corkish et al., 2002) and attempts by others (Berland, 2003; Kotter et al., 2008).

Researches are undertaking to improve nano-antenna for solar energy collecting. Coupled tunnelling diodes are one of the most significant parameter for nano-antenna. A few research groups are studying the utilization of nano-antennas for solar energy collecting. Antenna-based technologies differ from PV technologies. Antennas depend on resonance and physical geometries is a function of bandwidth whereas PV cells are quantum devices and limited by material band-gaps. Ideally, nano-antennas can be used to absorb light in the range between 0.4 and 1.6 μm wavelength because about 85 percent of the solar radiation lies in this region comparing to the longer, far-IR wavelengths (Berland, 2003; Kotter et al., 2008).

In order to capture mid-IR solar radiation, the US division of Energy's Idaho National Laboratory is trying to establish approaches by using nano-antenna technology. Different types of structures have been studied and a prototype has been developed which is made up of a 1.0 cm^2 array of gold nano-antennas. Naturally radiated solar power and earth radiated thermal power (electromagnetic radiation) is captured via nano-antenna elements. A standing-wave electrical current is produced in the antenna surface due to the incident of radiation and absorption take place at the antenna's resonant frequency. An alternating current is produces along the antenna surface at the same frequency of the resonance, during the resonance mode of operation of the antenna. This current induces due to the cyclic plasma movement of free electron along the antenna surface. The resonance frequency occurs at the THz frequency range of the nano-antenna.

The nano-antenna was made-up by growing rod-like arrays of gold material directly onto a silicon substrate. When light strikes the antenna surface, it excited the (Plasmon's

oscillating waves) electrons. These active electrons are then imported into the semiconductor over the Schottky barrier, thus generating a measurable photocurrent without supplying an external voltage. A serious benefit of the device is that the photocurrent is adequate to photons with energies above the band-gap of the semiconductor. In order to offer a novel technique of capturing and detecting IR photons, this result is significant because in the range of electromagnetic spectrum, the Plasmon resonance wavelengths are related in the near IR region of the electromagnetic spectrum. The shorter the nano-rods will provide shorter resonant wavelength.

2.4 Nano-antenna parameters

2.4.1 Design specification of conventional antenna in radio frequency

This section will briefly introduce some important parameters necessary for the RF antenna in order to characterize the performance of nano-antenna. The parameters includes return loss, impedance bandwidth, radiation pattern, directivity, antenna gain, antenna efficiency, input impedance, resonant frequency and bandwidth.

2.4.2 Return loss (RL)

The Return Loss (*RL*) is also known as reflection coefficient or S-Parameter (S_{11}). Actually, reflection coefficient represents the amplitude of reflection. The reflection coefficient is denoted by the symbol Gama, Γ. The voltage reflection coefficient is defined as the ratio of the reflected voltage amplitude to that of the forward voltage amplitude. When the unit of reflection coefficient is converted into the dB, then that reflection coefficient is representing as the return loss. The term that demonstrates how much amount of power is lost into the load and how much volume of power does not come back to the load after reflection is defined as the return loss or *S*-parameter (S_{11}). If the impedance of the transmitter does not match with the impedance of the load or receiver,

then the rate of reflection of inputted signal wave will be increased and the impact of this reflection will be more on the output. That means that portion of the input energy applied to the load will be returned back in the direction of the source instead of getting the load. These reflected waves are superimposed together with the incident wave to form the standing wave. On the other way, a standing wave can also be defined as the combination of waves moving backward and forward on the similar waveguide. Voltage Standing Wave Ratio (VSWR) is another factor that can also be described in terms of the voltage magnitude of the reflected voltage as well as the reflection coefficient. The ratio of the maximum to the minimum value of the voltage of the reflected wave is defined as the voltage standing wave ratio. The reflection co-efficient is given by the definition as,

$$\Gamma = \frac{V^-}{V^+} \tag{2.17}$$

Where V^- the amplitude of the voltage of reflected waves is moves towards source from the load and V^+ is the amplitude of the input voltage to load.

Reflection coefficient is also expressed in terms of the input impedance or characteristics impedance of the antenna and the impedance of the feeding source network. So, now reflection coefficient is also defined by,

$$\Gamma = \left| \frac{Z_{in} - Z_s}{Z_{in} + Z_s} \right| \tag{2.18}$$

Where, Z_{in} is the input impedance of the antenna and Z_s is the impedance of the feeding network.

Voltage standing wave ratio (VSWR) is expressed as a function of reflection coefficient.

$$VSWR = \frac{1+|\Gamma|}{1-|\Gamma|} \tag{2.19}$$

Hence the *RL* is a parameter similar to the Voltage Standing Wave Ratio (VSWR). The VSWR express how strong the matching among the transmitter and antenna has taken place. The *RL* is given as (Makarov, 2002):

$$RL = -20\log_{10}|\Gamma| \tag{2.20}$$

The value of Γ and *RL* are 0 and ∞ respectively for the antenna that's impedance is perfectly matched, which means no energy or power would be returned back. And all incident power of the antenna will be returned back towards the source if the value of Γ= 1 and *RL* = 0 dB that is the most worst for performing any kind of devices. More negative S_{11} implies a better reception of power by the antenna. In other words, more power is allowed to pass through from the input. Table 2.1 displays the different values of return loss and its corresponding reflected and absorbed portion of the input power for understanding the importance of return loss more easily.

Table 2.1: Percentage of Reflected Power with S_{11}

S_{11} [dB]	Reflected [%]	Pass through [%]
0	100	0
-10	10	90
-20	1	99
-30	0.1	99.9
-40	0.01	99.99

2.4.3 Impedance bandwidth

The bandwidth is generally defined as the range of frequencies at which the voltage standing wave ratio is not greater than 2 that is equivalent to a return loss of -10 dB or 10 % reflected energy or power. Sometimes the requirement of VSWR should be less than

1.5 for meeting with the particular applications which is equal to a return loss of -14 dB or 96% passed power. In other way, Voltage Standing Wave Ratio (VSWR) or the variation of input impedance with frequency and quality factor (*Q*-factor) of the antenna could also be used to define the bandwidth. The *Q*-factor is described as a measurement of the bandwidth of an antenna that is related to the center frequency of bandwidth. If the antenna functions over a frequency band between f_l and f_u with middle frequency $f_c = (f_l+f_u)/2$, then the *Q*-factor is defined by:

$$Q = \frac{f_c}{f_u - f_l} \tag{2.21}$$

Where f_l = lower cut-off frequency and f_u = upper cut-off frequency.

There is an inverse relationship between the bandwidth and the *Q*-factor. That means that the more the value of *Q*-factor, the lower the value of bandwidth and also vice-versa. Actually, *Q* signifies the losses related with the antenna. Usually there are surface wave, radiations, conduction (ohmic), and dielectric losses. The losses owing to surface waves are very minor for very thin substrate and it can be ignored. However, the rate of surface wave losses will be increased as the thickness of substrate increases. The big portion of the total power supplied from the source releases as the surface wave. This contribution of surface wave is regarded as an undesirable power loss because it is basically distributed along the sides of dielectric that degrades the antenna performance. So, the impedance bandwidth of a nano-antenna can be related with *Q*-factor by the Eqn. (2.22) given below.

$$BW = \frac{VSWR - 1}{Q\sqrt{VSWR}} \tag{2.22}$$

It is also possible to express impedance bandwidth as a function of parameters of antenna's radiation such as gain, directivity, side-lobe levels, and half power beam width within definite limits. The percentage impedance of a nano-antenna can be found out by

taking the percentage of the ratio of the difference between f_l and f_u to the center frequency. So, the percentage impedance bandwidth is defined by Eqn. (2.23) .

$$\%BW = \frac{f_u - f_l}{f_c} \times 100\% \tag{2.23}$$

2.4.4 Radiation pattern

The radiation pattern is one of the most important performance parameter for any type of antenna. The main function of the antenna is to receive or transmit power. The radiation pattern is describe as "a mathematical function or a graphical illustration" of the radiation properties of an antenna. It also represents as a function of the spherical radial distance and angular position from the antenna. This plot is done in spherical coordinate system. Angular position is identified by the azimuth angle φ and the elevation angle θ. Radial distance is expressed as the radius of a sphere formed by radiated or received power. More exactly it is defined as the plot of the power give out from an antenna per unit solid angle that is also named as the radiation intensity (Balanis, 2012).

2.4.5 Directivity

The directivity D of an antenna is defined as the ratio of the maximum radiation intensity to the average radiation intensity. In the branch of electromagnetics, directivity is called the figure of merit of an antenna. It indicates how much amount of energy is radiated in one direction with respect to the power radiated of ideal antenna. An ideal antenna or isotropic antenna is one that can radiate power uniformly in all directions. How much power is radiated in one specific direction is defined by the term radiation intensity (Balanis, 2012). In another way, the directivity of a practical or antenna is equal to its radiation intensity of non-isotropic source in a given direction, compared to that of an isotropic source.

$$D = \frac{U}{U_0} = \frac{4\pi U}{P_{in}} \tag{2.24}$$

Where,

D is the directivity of the antenna

U is the radiation intensity of the antenna

U_0 is the radiation intensity of an isotropic source

P_{in} is the total power radiated

2.4.6 Antenna gain

The antenna gain is one of the most significant antenna design criterion. The antenna gain G, is defined as the ration of radiation intensity to input power divided by 4π. The gain can be expressed by the following equation:

$$Gain = 4\pi \frac{u(\theta, \phi)}{Pin} \tag{2.25}$$

The directivity is defined by how much an antenna can focus power in one direction corresponds to the radiation in any other directions. The directivity of an antenna gain will be equal to the gain of the antenna if the antenna has no loss that means efficiency of an antenna is 100%. But it is very difficult to get that type of antenna practically. Then, that antenna is called as an isotropic radiator. Therefore the gain of an antenna is the total volume of power which can be attained in one direction at the expenditure of energy lost in the all other directions as explained by Ulaby (Ulaby, Michielssen, & Ravaioli, 2010).

2.4.7 Antenna efficiency

The efficiency of an antenna can be described as the ratio of actually radiated power to the input power at the terminals of the antenna. If the radiated power is P_{rad} and the total input power is P_{in} then we can express their relation by the following equation

$$P_{rad} = e_{cd} \times P_{in} \tag{2.26}$$

The total amounts of losses at the edges of the antenna and within the antenna geometry are taken into account for describing the antenna efficiency. These losses are given by (Balanis, 2012) as:

1. Reflections due to mismatch between the antenna and the transmitter
2. I^2R losses (dielectric and conduction)

The efficiency can be calculated by the following equation:

$$e_{cd} = \frac{R_r}{R_r + R_L} \tag{2.27}$$

e_{cd} is indicates antenna radiation proficiency. The radiation efficiency is defined as the ratio of the power delivered to the radiation resistance R_r, to the power delivered to R_r and R_L.

2.4.8 Input impedance

The ratio of the voltage at the input ends to the current at the input ends is represents input impedance. Input impedance of an antenna also defined as the ratio of suitable component of electric field to the exact component of magnetic field at the same input ends. So, it is written as:

$$Z_{in} = R_{in} + jX_{in} \tag{2.28}$$

Where Z_{in} is the input impedance of antenna

R_{in} is the input resistance at the input ends of antenna

X_{in} is the input reactance at the input ends of antenna

R_{in} is the real part and X_{in} is the imaginary part. Reactance part, X_{in} of antenna, signifies how much power stored in the near-field. There are two components in the resistive part, R_{in} . One is loss resistance, R_L and another is radiation resistance, R_r. R_L indicates the total dissipated power in the antenna that is lost as heat. This loss is done due to conductive and dielectric material. The power related to the R_r specifies about the total actual power radiated from the antenna.

2.4.9 Resonant frequency and bandwidth

Usually, an antenna can successfully function at a range of frequencies centered by a specific resonant frequency. Some antenna has multiple resonant frequencies instead of single resonant frequency. Resonant frequency and electrical length of an antenna are interrelated which can be calculated physical length divided by the velocity factor. At the resonance frequency, the antenna will offer much superior coupling of the EM waves to radiate. The bandwidth can be defined as the frequency region in which the performance of the antenna conforms to a specific standard with respect some characteristics (For example bandwidth, input impedance, pattern, polarization, gain, efficiency etc) are within an acceptable value of those at the center frequency. Wider bandwidth antenna is expectable but wider bandwidth antenna provides much lower directivity comparing to the narrow band antenna. Resonant frequency and bandwidth can be changed with the adjustment of critical dimensions of the antennas and the feeding networks.

2.5 A technical review of recent works in energy harvesting

The demand for energy is increasing day by day with the growth of the world's population. The reserves of fossil fuel are limited and have a detrimental effect on the environment, which suggests further research activities for exploiting alternate renewable energy resources. The deleterious effects due to combustion of fossil fuels and limitation of solar cell also suggests alternate renewable energy resources. It is observed that about 85% of energy are laying in the visible and infrared region of the solar spectrum. Although there are a lot of renewable energy sources, solar energy is one of the most promising among them (J.-M. Wang & Lu, 2013). Hua yu et al. proposed a hybrid energy scheme from the ambient light and vibrational energy (Yu, Yue, Zhou, & Wang, 2014). Energy can also be harvested from the counter balancing movement in bicycle riding (Yang, Yeo, & Priya, 2012). In 1964, William Brown primarily established the rectenna systems (Brown, 1976). In order to progress the invention, a significant study was conducted to find out the microwave rectenna devices (McSpadden, Yoo, & Chang, 1992; Suh & Chang, 2002). Now-a-days, nano-antenna is a very widespread technology due to their capability to confine incident electromagnetic fields in sub-wavelength volumes (Feichtner, Selig, Kiunke, & Hecht, 2012; McMahon, Gray, & Schatz, 2010). Optical properties of nano particle were the main focusing point of the researcher during the last 15 years (Gotschy, Vonmetz, Leitner, & Aussenegg, 1996; Kottmann, Martin, Smith, & Schultz, 2000; Nehl, Liao, & Hafner, 2006; H. Wang, Brandl, Le, Nordlander, & Halas, 2006). M. Bozzetti et al. (Bozzetti et al., 2010) proposed a spiral structure antenna printed on a substrate of 18×18 μm^2 with the ground plane and antenna thickness of 150 nm where maximum E-field and output current are 62525 V/m and 0.03 mA, respectively. Another four square spiral antenna has been proposed in (Gallo, Mescia, Losito, Bozzetti, & Prudenzano, 2012) with the performance of 3.8 µA output current at 28.3 THz in order to harvest the thermal energy, which is provided by the sun and re-emission from the

earth. This spiral antenna (Gallo et al., 2012) array consisted of gold printed on a SiO_2 substrate, which was illuminated by a circularly polarized plane wave.

The radiation efficiency is an important parameter of the optical energy harvesting system in the visible and infrared region. Metal and antenna dimensions have a major effect on the radiation efficiency. The variation of the radiation efficiency of Silver (Ag), Gold (Au), Aluminum (Al), Copper (Cu) and Chromium (Cr) has been reported in (Vandenbosch & Ma, 2012). Silver (Ag) has shown the radiation efficiency of 90% and solar power harvesting efficiency of 60-70 %, which are the highest among all the metals. The efficiency of the nano-rectenna system depends on two major factors which are light and rectifier. Light is captured by the antenna systems to be carried into its terminals and the rectifier is used as a converter to get usable low frequency power from the extracted high frequency power. The efficiency of the rectenna also depends on the perfect matching between the rectifier and the antenna. Matching efficiency between the dipole and the rectifier was extensively and numerically investigated and it was observed that maximum matching efficiency of 97% and 57% can be reached for Ag and Al, respectively, where single linearly polarized dipole can deliver a maximum power in the order of 5-10 pW (Ma & Vandenbosch, 2013a). An optimization of the geometrical parameters (2.9 μm spacing between the arrays, line width of 50 nm, and the gap between the bow-tie of 25 nm) for terahertz energy harvesting bow-tie nano-antenna based nanoarray has been simulated utilizing the finite element method (Sabaawi et al., 2013). In order to improve the harvesting efficiency, an elliptical shaped nano-antenna (Hussein, Areed, Hameed, & Obayya, 2014) with air gap has been simulated in the wavelength range of 400 nm to 1400 nm. When the sun is fully irradiated, it shows the 74.6% efficiency at 500 nm, which provides better efficiency compared to conventional solar cell for a particular wavelength. An antenna integrated with a rectifier was proposed in

(Gadalla et al., 2014) along with the impedance matching. Optical or nano-antenna represents light coupling devices, combined of single or multiple nano-meter-scale metallic particles. Recently, nano-antenna employs a novel idea and extensive interest in the optical region comparing with the traditional radio-frequency antennas. When a light source impings the surface of the nano-antenna, the close-field surface plasmon (SP) resonance occurs (Wu, Li, & Liu, 2010).

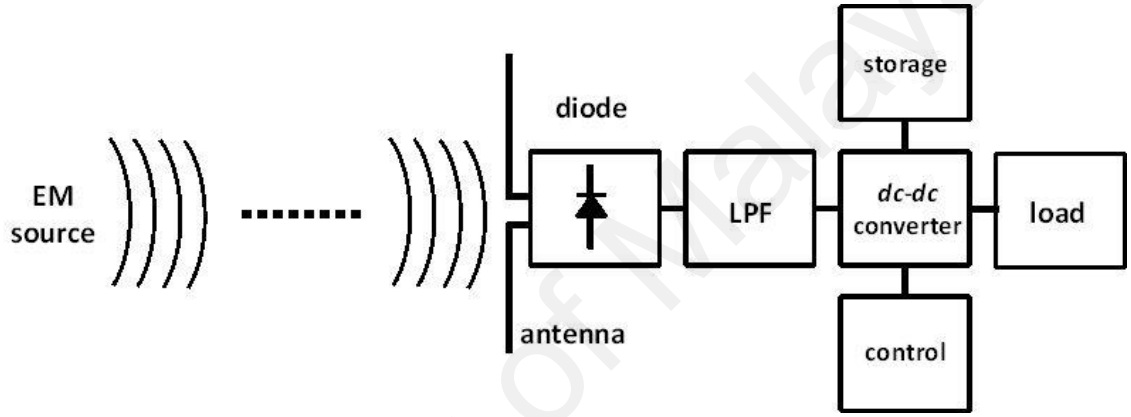

Figure 2.2: Schematic block diagram of 'rectenna' system in order to energize the load (Ref:www.intechopen.com/books/).

Surrounding the antenna, highly localized field is produced due to the SP excitation, such as a metal tip was extensively employed to obtain local-field improvement and custody in the microscopy (Sánchez, Novotny, & Xie, 1999). Below the diffraction limit, bow-tie nano-antenna was confirmed to be active in embracing the spatial resolution (Grober, Schoelkopf, & Prober, 1997). Similarly, C-shaped metallic structure apertures were also investigated due to the high transmission (Shi, Hesselink, & Thornton, 2003). Field enhancement of the nano-antenna is tremendously reliant on its geometrical configuration. Thus, different structural design in the range of single (Chen, Li, Taflove, & Backman, 2006; Kattawar, Li, Zhai, & Yang, 2005) to delicately organize nano particles including couple and arrays (Genov, Sarychev, Shalaev, & Wei, 2004;

Sundaramurthy et al., 2005), are reported. Near closed dual nano particles exhibit much better SP improvement than a single nano particle among the all designs. The bow-tie nano-antenna (nanoparticle pairs) provides respectable field imprisonment.

The geometrical effects, such as length and gap effects was successfully fabricated in experiment (Sundaramurthy et al., 2005). Optical antenna can be used as an effective substitute of the commercial solar panel due to its low conversion efficiency and high dependency on the weather condition. In order to generate electricity from the sun and earth re-emitted sun's energy with high conversion efficiency, one of the possible solution is the use of the rectenna (a structure constitute by an antenna and a rectifier) consist of a microwave antenna, a low pass filter (LPF), a rectifier diode and a DC pass filter illustrated in Figure 2.2 (Heikkinen & Kivikoski, 2003; Park, Han, & Itoh, 2004). Filter removes the reflected higher order harmonics and allows passing of the generated THz signal. In order to convert the AC power into DC, a rectifier diode is used.

The major technological limit of the rectenna is the high power loss due to results of the parasitic capacitance (junction capacitance) at the p-n junction diodes during the operation at high frequency. Another difficulty of the recetnna system is the fabrication as it requires e-beam lithography technique. Typically, when the extremely fine resolution is needed, use of the e-beam lithography is suggested in (Krishnan, La Rosa, Stefanakos, Bhansali, & Buckle, 2008). Compared to the conventional photovoltaic cell, the optical antenna provides a wider spectrum of light that it can receive. Nano-antenna array has been used for energy harvesting (Bareiss et al., 2011). Slotting effect of patch antenna with 60% and 36% size and resonance frequency reduction have been achieved respectively (Bhunia, 2012). A comparative study of different types of antenna has been given in (Kocakarin & Yegin, 2013). A numerical simulation of spiral nano-antennas for

improved energy harvesting is studied in (Briones, Briones, Cuadrado, Murtry, et al., 2014). Another flower shaped dipole nano-antenna is proposed in (Hussein et al., 2014) that achieved maximum efficiency of 74.6% at the maximum irradiance of the sun.etween the antenna and rectifier thin film diode to harvest the infrared THz energy.

In this work, a novel circular edge bow-tie nano-antenna is proposed and designed for energy harvesting by using 3D-electromagnetic solver. The slotting effect is investigated in designing circular edge bow-tie nano-antenna for this energy harvesting system. The proposed antenna consists of two circular edges triangular shaped thin film of gold, printed on a SiO_2 substrate with the ground at the bottom plane. The Lorentz-Drude model is used to analyze the behavior of gold at infrared frequencies. The proposed antenna is targeted to collect the re-emitted earth radiation and the radiation from the infrared region which can be converted into electricity. The performance of the proposed antenna is investigated in terms of the electric field (V/μm) and captured radiation bandwidth.

2.6 Summary

In this chapter, an up to the date literature review on nano-antenna for energy harvesting work has been presented. By critically analysing various works, there have been raised several issues of concerning mechanical limitations and novelty in geometrical design of nano-antenna for energy harvesting application have been raised. As observed, the geometrical design is greatly affected by resonance frequency, frequency of operation in THz, electric field intensity (V/μm), bandwidth, return loss, voltage standing wave ration etc., which in turns sets the bottleneck in the system's performance. So, designing a nano-antenna holds a lot of importance to meet up with certain features for energy harvesting application. This chapter also describes the fundamental ideologies of nano-antenna theory as it is important and can be further applied to our illustration of nano-antenna

design and analysis. The typical antenna parameters such as antenna bandwidth, resonance frequency, radiation pattern, antenna gain, directivity, etc. is placed with emphasis. As a result, to evaluate the nano-antenna performance as comparing to the existing RF antennas we can take them as reference. Based on the study, the idea of nano-antenna for energy harvesting at the optical frequency will be further developed in the following chapters.

CHAPTER 3: METHODOLOGY

3.1 Antenna design methodology

The choice of suitable effective frequency band for designing the antenna proposed in this work lies in terahertz frequency and far infrared region. The antenna must be designed to have its size as small as possible for applying in a compact receiving antenna. Ground plane size will have to take into account for calculating the overall size of the antenna. However, there is a trade-off relation between the performance of the antenna and antenna geometry. Furthermore, directivity is also the important factor to analyse the performance of the receiving nano-antenna. Therefore, the individual receiving antenna is to be directed in a way that its main lobe is leaded to the transmitter, which helps to improve the amount received energy.

This antenna is designed for energy harvesting applications. The resonant frequency *fr* and substrate material with proper dielectric constant, and thickness are first selected to evaluate the dimension of the antenna. The 1.2 μm thick substrate used for this antenna has used SiO_2 as material which has a dielectric constant of 4.86. The resonant frequency picked for this antenna is 25.3 THz for the application of energy harvesting from far infrared region. This antenna contains a large circular edge, followed by two triangular shaped, microstrip feeding line used as a feed line and a ground plane with a much smaller width at the bottom side of the substrate.

The proposed antenna consists of circular edges bow-tie gold structure is printed on a substrate of 18×18 μm^2 with the thickness of 1.2 μm. Ground plane and circular edges bow-tie part 1 and part 2 consist of gold film with a thickness of 150 nm. 3D Electromagnetic Simulator has been used in order to design the proposed antenna

structure and perform the numerical analysis. This novel design of the proposed antenna is capable of concentrating the electric field in the central of the gap of the bow-tie. This field is then transferred by a feeding line and converted into electricity in order to supply the load.

This novel antenna is designed with the intention of harvesting the electromagnetic radiation. This antenna has been investigated and analysed with a circularly polarized plane wave. In this simulation, hexahedral mesh grid is considered where the density of the mesh is determined by the cell size and cells per wavelength are given as 20. The number of mesh cells is measured as 85 million, which takes around 17-20 hours (with 3.4 GHz processor speed and 8 GB RAM). Excitation of surface Plasmon oscillation occurs due to the impinges of visible or infrared light on the antenna surface which results in a creation of hot spot where the field intensity is enlarged and drives the current toward the feeding point of the antenna (Ma & Vandenbosch, 2013b; H. Wang et al., 2006). By using this feature, antenna can be designed and broadened its field of application in nano scale imaging and spectroscopy (Bachelot, Gleyzes, & Boccara, 1995; Novotny, 2007), improvement of solar cell efficiency (Catchpole & Polman, 2008; Derkacs et al., 2008), and co-herent control (M. Stockman, Faleev, & Bergman, 2002; M. I. Stockman et al., 2004). Earth is cooler as compared to the sun and hence emits radiation of lower intensity. A black body is considered as an absorber that absorbs all incoming radiation and releases temperature dependent radiation spectrum. Let the black body radiation emitted power is consider as I and per unit area temperature is *T*. If c is the speed of light and λ is the wavelength, then the Planck's low spectral irradiance can be stated as (Planck, 1910).

$$\mathrm{I}(\lambda,\mathrm{T}) = \frac{2\pi c^2 h}{\lambda^5} \times \frac{1}{\exp\left(\frac{hc}{\lambda\kappa\mathrm{T}}\right) - 1} \tag{3.1}$$

Where h = Plank constant and κ = Boltzmann constant.

Over the frequency spectrum, the total power and the emitted radiation per unit area of a black body at temperature T is given by the following the equation (Gallo et al., 2012):

$$R(\mathrm{T}) = \int_{\circ}^{\infty} \mathrm{I}(\lambda, \mathrm{T})\, \mathrm{d}\lambda = \sigma \mathrm{T}^4 \tag{3.2}$$

If the scattering, extinction and absorption cross-sections consider as C_{sca}, C_{ext} and C_{abs} respectively then the nanoparticles optical radiation efficiency, η_{rad} is defined by Eqn. (3.3) (Dmitruk, Malynych, Moroz, & Kurlyak, 2010).

$$\eta_{rad} = \frac{C_{sca}}{C_{ext}} = \frac{C_{sca}}{\mathrm{C_{sca}} + \mathrm{C_{abs}}} \tag{3.3}$$

The total harvesting efficiency of the antenna is given by Eqn. (3.4) (Briones, Briones, Cuadrado, Martinez-Anton, et al., 2014).

$$\eta_{tot} = \frac{\int_{0}^{\infty} \mathrm{P}(\lambda, \mathrm{T}) \times \eta_{\mathrm{rad}}(\lambda)\, \mathrm{d}\lambda}{\int_{0}^{\infty} \mathrm{P}(\lambda, \mathrm{T})\, \mathrm{d}\lambda} \tag{3.4}$$

According to the Lorenz Drude (LD) model (Rakić, Djurišić, Elazar, & Majewski, 1998) the permittivity, ε_r can be expressed by the following equation:

$$\varepsilon_r(\omega) = \varepsilon_{\mathrm{r}}^{f}(\omega) + \varepsilon_{\mathrm{r}}^{\mathrm{b}}(\omega) \tag{3.5}$$

Where,

$$\varepsilon_r^f(\omega) = 1 - \frac{\Omega_P^2}{\omega(\omega - i\Gamma_0)} \tag{3.6}$$

$$\varepsilon_r^b = \sum_{j=1}^{k} \frac{f_j \omega_P^2}{\left(\omega_j^2 - \omega^2\right) + i\omega\Gamma_i} \tag{3.7}$$

The simplified drude model has also been considered to derive the Eqn. (3.8).

$$\varepsilon(\omega) = \varepsilon_\infty - \frac{\omega_P^2}{\omega^2 + \omega_\tau^2} + i \frac{\omega_P^2 \omega_\tau}{\omega^3 + \omega\omega_\tau^2} \tag{3.8}$$

The influence of the bound electrons to the relative dielectric constant is represented by the ε_∞. Here, ω_p represents the plasma frequency and ω_τ is the damping frequency. K Indicates the number of oscillators with frequency ω_j, strength lifetime is $\frac{i}{\Gamma_j}\Gamma_0$ indicates damping constant and Ω_p indicate intra band plasma frequency. Figure 3.1 demonstrates the geometric structure of the circular edge bow-tie nano-antenna indicating its each element and Figure 3.2 it shows the complete basic structure of the antenna with labelling all parameters. By performing a number simulations the optimized dimensions of the antenna geometry have been achieved and are reported in Table 3.1.

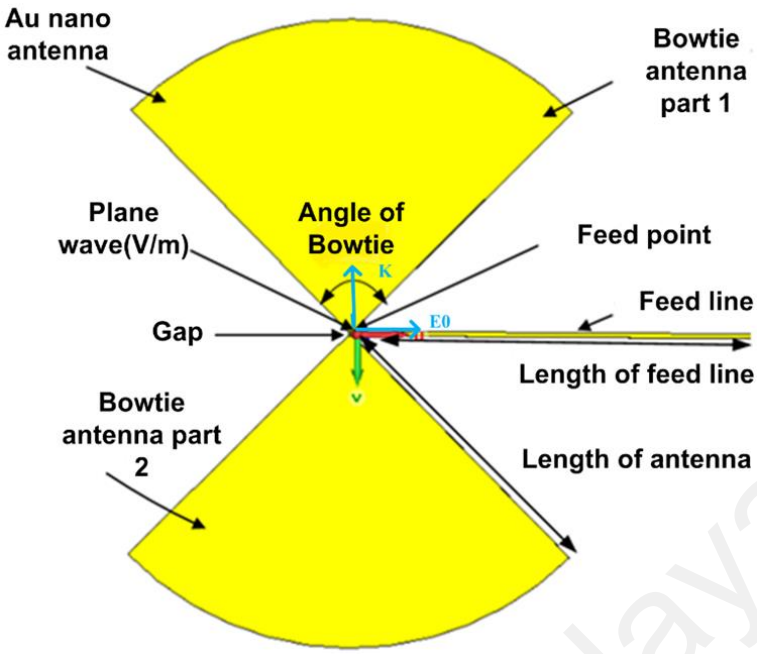

Figure 3.1: Geometry structure of the circular edges bowtie nano-antenna.

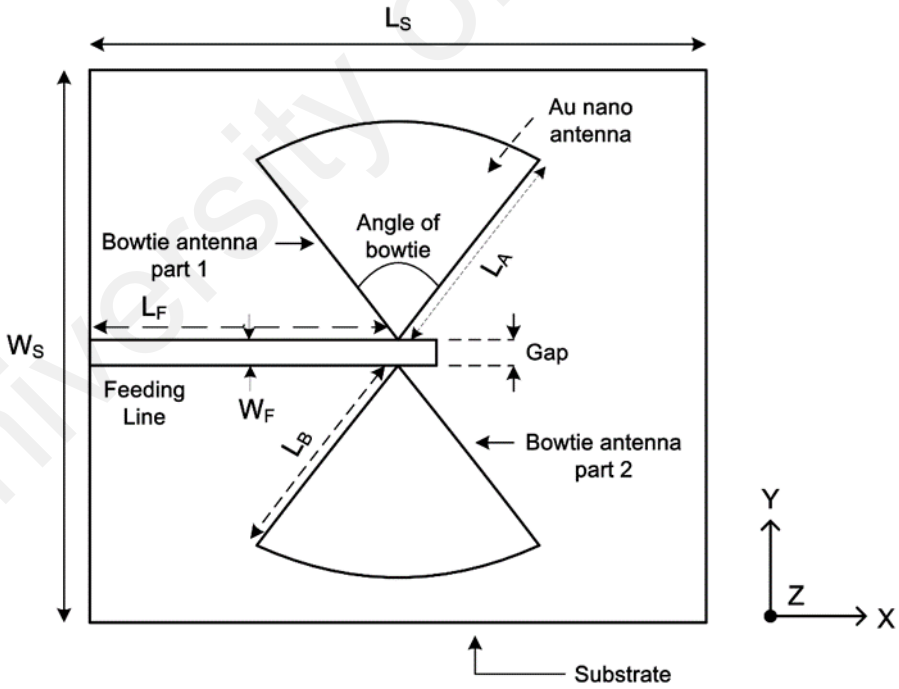

Figure 3.2: Complete basic configuration of the antenna with labelling all parameters.

Table 3.1: Optimized dimensions of the antenna geometry.

Antenna Configuration	**Variables of the Parameters and Dimensions (µm)**		
Substrate	L_s	W_s	t_s
	18	18	1.2
Antenna	L_A	L_B	t_A
	5.93	5.93	0.150
Ground plane	L_g	W_g	t_g
	18	18	0.150
Feed line	L_F	W_F	t_F
	9	0.11	0.150
Gap	L_{gap}	W_{gap}	t_{gap}
	0.05	0.05	0.150

3.2 Design initialization

The finite difference time domain method (FDTD) using computer simulation technology (CST) microwave studio was used for the simulations to calculate the terahertz response of proposed nano-antenna. The real and imaginary parts of the gold dielectric function are obtained from LD model. The structures are illuminated from above, perpendicular to the antenna long axis. The gap between the nano-antenna represents an essential feature of the antenna structure. To characterize the spectral response of the antenna and its intensity enhancement, we therefore calculate the field intensity inside this gap in relative units to the illumination intensity. We first investigated antenna resonances and the local field intensity enhancement between the bow-tie tip of the designed antenna. The designed antenna formed by two identical circular edges bow-tie shaped (with radius R = 5.93 µm) of dielectric function $\varepsilon_r(\omega)$, separated by a gap g. The geometry of the antenna strongly influences its optical properties. This antenna is designed for energy harvesting

applications. The resonant frequency *fr* and substrate material with proper dielectric constant and thickness are first selected to evaluate the dimension of the antenna. The 1.2 µm thick substrate used for this antenna has used SiO_2 as material which has a dielectric constant of 4.86. The dielectric constant has been consider at the optical constant. The resonant frequency picked for this antenna is 25.3 THz for the application of energy harvesting from far infrared region. This antenna contains a large circular edge, followed by two triangular shaped, microstrip feeding line used as a feed line and a ground plane with a much smaller width at the bottom side of the substrate. The designed antenna three dimensional view is given in Figure 3.3. To validate the simulation results, initially the conventional spiral antenna shown in Figure 3.4 has been considered and a brief description and re-produced results provide in the following section.

3.3 Simulation results

Firstly, the structure of antenna is designed by the high frequency electromagnetic solver which is the most popular antenna design simulation software, CST Microwave Studio 2012 (Studio). This Microwave Studio CST software constructed on Finite Difference Time Domain (FDTD) solver is regarded as one of the most technically advanced software for three dimensional electromagnetic simulations. A key feature of CST is that it allows the input of parameters to specify the exact dimensions of the antennas which is useful because:

1. This software allows the user to change the dimension later, which gives flexibility in designing the antenna.
2. It helps to study the effects of one specific parameter to antenna performance, also known as parametric study.

Different types of antenna can be designed with the help of CST software. Antenna (planner) has been selected among all antenna configurations to create the new project from where antenna design was being started. Gold is chosen as the material to obtain the most accurate results as possible.

The three dimensional view of the antenna designed in CST is shown in Figure 3.3. The yellow color of the designed antenna in CST indicates that the conducting material used for this design is gold.

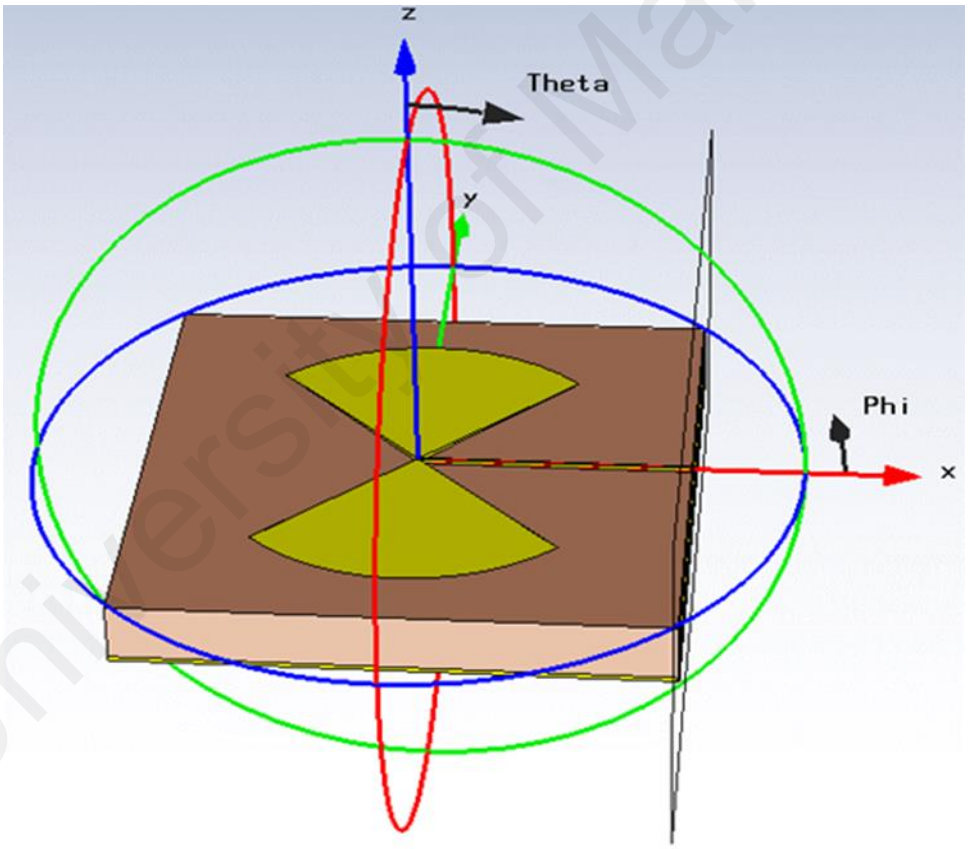

Figure 3.3: Three dimensional geometric structure of circular edges bow-tie nano-antenna.

Figure 3.2 shows the geometric structure of the circular edges bow-tie nano-antenna indicating its each element. The total length of the antenna is around 11.86 μm. This

antenna is capable to capture and transform the ample power from earth radiation and is also able to collect solar energy in the infrared frequency region. The nano-antenna is illuminated by the circularly polarized plane wave with a 1000 V/m E-field magnitude. Figure 3.3 shows the three dimensional geometric structure of circular edges bow-tie nano-antenna. The yellow trace indicates gold nano-antenna and the feeding line. The bright gray indicates the substrate consists of SiO_2 with thickness of 1.2 μm. The width and length of the feeding line 110 nm and 9 μm.

To validate the simulation results in this study, initially the conventional spiral antenna shown in Figure 3.4(a) is considered as a reference antenna where the results in Figure 3.4(b) and Figure 3.4(c) are reproduced (Gallo et al., 2012). This conventional spiral antenna consists of 18.9×18.9 μm^2 substrate with 1.2 μm thickness. The ground plane and the antenna arms are structured by the gold film having thickness 150 nm.

The electromagnetic field of the designed antenna is captured through the waveguide port that is applied into the feed point of the feed line. Mesh properties are defined under Global Mesh Properties, which specifies accuracy of the simulation by cutting the model into many infinitesimal parts. There are many types of solver to run the simulation. The transient (time-domain) solver in CST is the general solver which is capable to solve electromagnetic field problems at the greater range of frequencies. The type of mesh used here is hexahedral and accuracy set for simulating this antenna is -40 dB. However, there are also some specialized solvers that will show much better performance for some specific applications while the same high level of accuracy has been maintained. For our purpose of simulating this nano-antenna, transient solver is the most appropriate solver. To improve the original design, different parameters of the design can be modified to see its effect on the return loss and bandwidth by means of CST software but this may need

a prolonged simulation time. The designed antenna's features and performance have been estimated, optimized, and accomplished by CST Microwave Studio 2012.

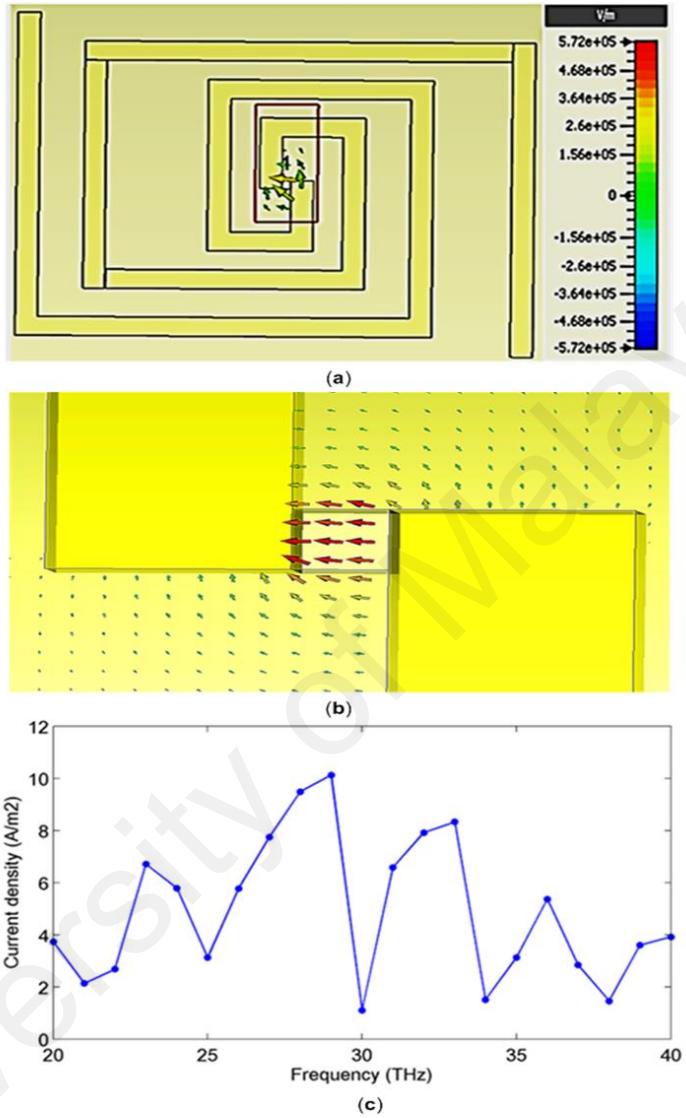

Figure 3.4: Conventional Spiral nano-antenna. (a) Conventional spiral structure and Maximum electric field scale indicate at the gap of the nano-antenna. (b) The E field-line in the gap of the rectenna. (c) Reproduce response of the antenna to a plane wave excitation versus the frequency when a resistor is connected at the micro strip line input (Gallo et al., 2012).

3.4 Summary

In this chapter, a complete theoretical design procedure of the proposed circular edge bow-tie nano-antenna has been presented. The circular edge bow-tie antenna is designed with the intention of harvesting the electromagnetic radiation from the sun and earth. Simulation study has been accomplished by feeding the nano-antenna with a microstrip line fixed into the substrate to determine radiation characteristics and this is analysed with a circularly polarized plane wave. But, nano-antenna performance can also be affected in certain ways with the excitation and substrate materials. These will be investigated in the succeeding chapters. The dispersive characteristics of gold materials as the substrate have been described through the use of the Lorentz-Drude model. A few essential discussions for the simulation setup are also included in this chapter for reader's accomplishment. The optimized substrate thickness of the bow-tie nano-antenna is considered as 1.2 μm with permittivity of 4.86 as proposed dimensions is optimized by performing a number of simulation. The gap between the bow-tie tips is calculated as 50 nm and the feeding line thickness is 110 nm as found from well given responses in terms of some antenna parameters such as return loss, operating bandwidth and voltage standing wave ratio etc. Finally, this chapter has described the process of optimization for the designed antenna by using the 3D electromagnetic solver.

CHAPTER 4: RESULTS AND DISCUSSION

In this chapter, all the responses obtained from the designed antenna are presented sequentially where the several effects of influential factors are also shown.

4.1 Return loss and impedance bandwidth

In this work, a bow-tie circular edged antenna with a rectangular air gap has been considered. The proposed antenna is made by gold printed on the 18×18 μm^2 substrate, having permittivity of 4.86 and thickness of 1.2 µm. At optical frequency, metallic properties of the metal are very significant. In order to accurately model the antenna features, the frequency dependency of the materials permittivity is very necessary. The dispersive behaviour of the gold material has been analysed by the Lorentz-Drude (LD) model.

The simulated return loss of the novel circular edges bow-tie nano-antenna has been shown in Figure 4.1 for different feeding line thickness. The proposed antenna provides better performance around the frequency 25.3 THz with a feeding line thickness of 110 nm. From the Figure 4.1, it can be seen that the return loss value below -10 dB from 23.2 THz to 27 THz (Bandwidth 3.8 THz) and from 31 THz to 35.9 THz (Bandwidth 4.9 THz). This feature helps to capture the radiation in a wider frequency range in order to harvest energy from the earth radiated and infrared band. From the simulation result, it can be observed that the value of maximum directivity is 8.57 dBi.

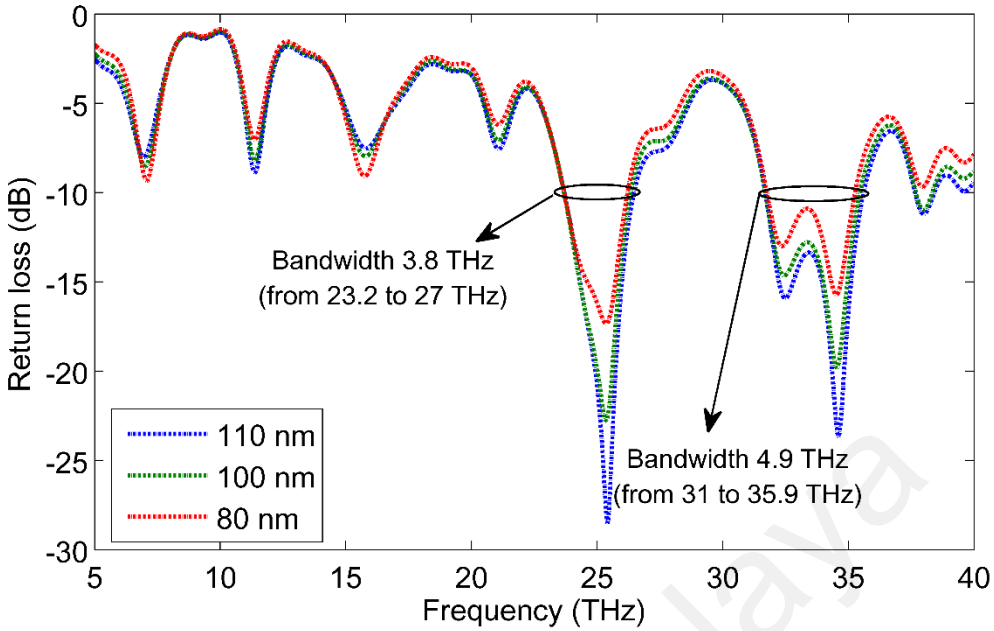

Figure 4.1: Variation of the return loss versus frequency for different feeding line thickness.

In order to evaluate the electric field intensity, best fitted return loss and larger bandwidth, a number of simulations were investigated. During the simulation, the antenna is illuminated by 'circularly' and 'linearly' polarized plane wave separately to capture the maximum electric field from the infrared band and as well as from earth radiation. The electromagnetic investigation was performed from 5 THz (60 µm) to 40 THz (7.5 µm). The performance of the circular edged bow-tie nano-antenna is measured in terms of captured electric field from the gap and transferring it through the feeding line from the end of the feeding line. As observed, the maximum electric field intensity has been found at the centre of the bow-tie gap and this electric field has been transferred by feeding line. Along the antenna structure the free electron of gold flows toward the feed point and concentrated at the gap. Figure 4.2 illustrates the radiation patterns at the frequency of 25.3 THz. Half power beam-width is also an important matter in order to capture energy from different directions. In this design, the half power beam-width is large enough in order to capture infrared energy as well as thermal energy from different directions.

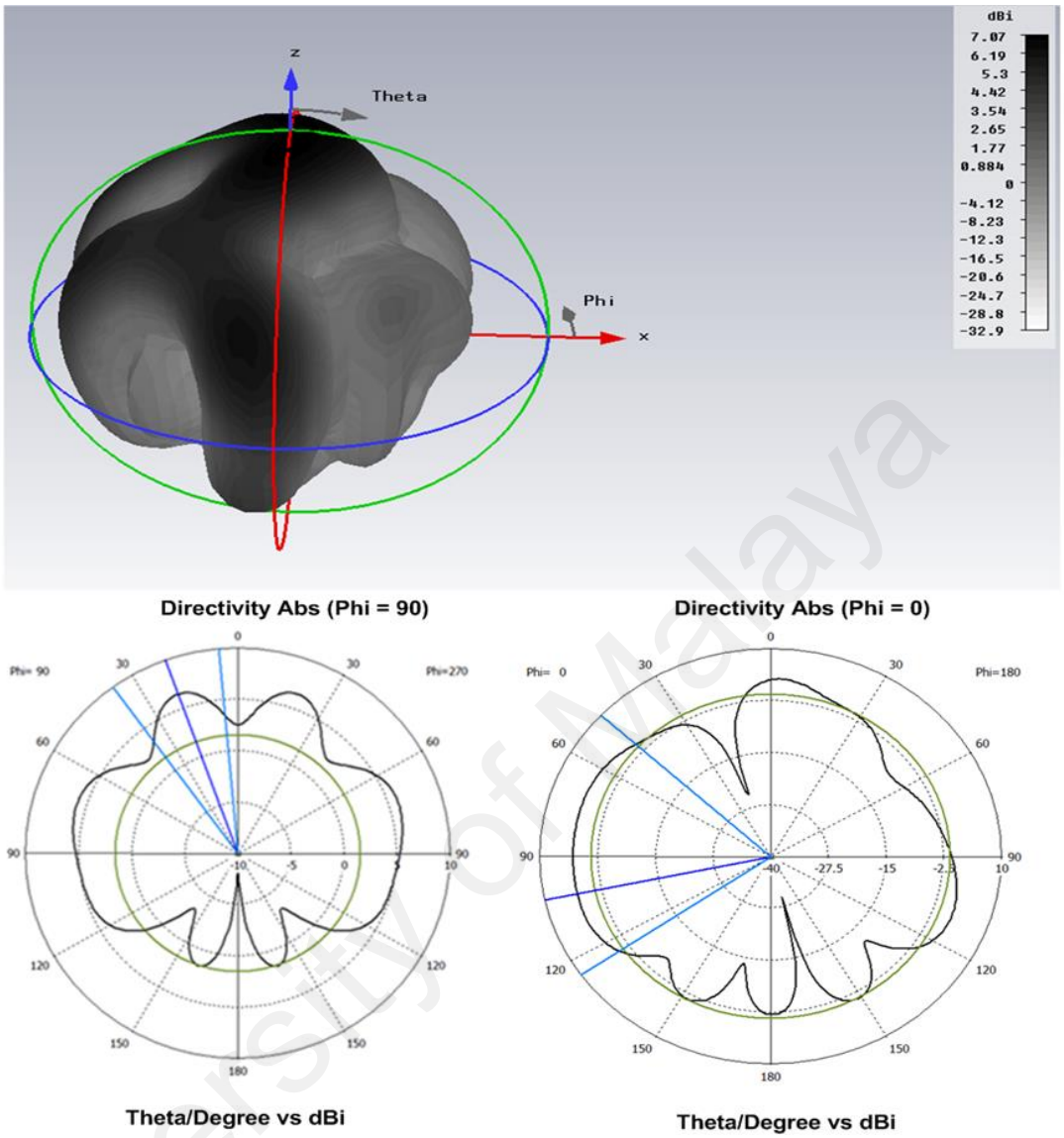

Figure 4.2: Simulated 3D and 2D radiation pattern of the circular edges bowtie nano-antenna.

From the single antenna structure, the electric field waveform across the gap between the antenna elements has been simulated and analysed. Figure 4.3 shows the measured electric field versus frequency for a circular polarized plane wave, excited with a fundamental frequency of 25.3 THz with a frequency sweeping range from 5 to 40 THz. This antenna shows a steady response between 31 THz to 35.9 THz along with a maximum value at 25.3 THz as seen in Figure 4.1. The electric field intensity can be

increased by making an array of the antenna, but due to coupling effect, the antenna efficiency will be decreased. In order to overcome the coupling effect of the antenna array, it is also required to improve the device efficiency by selecting a proper design, geometrical structure optimization, etc. The value of electric field is decreased due to connecting the feeding line, but it will be able to recover the loss by enabling the array for further efficient performance. Electric field can be concentrated in a common gap with the help of the feeding line from the array and single rectifier is needed to operate the whole array instead of one rectifier per single element.

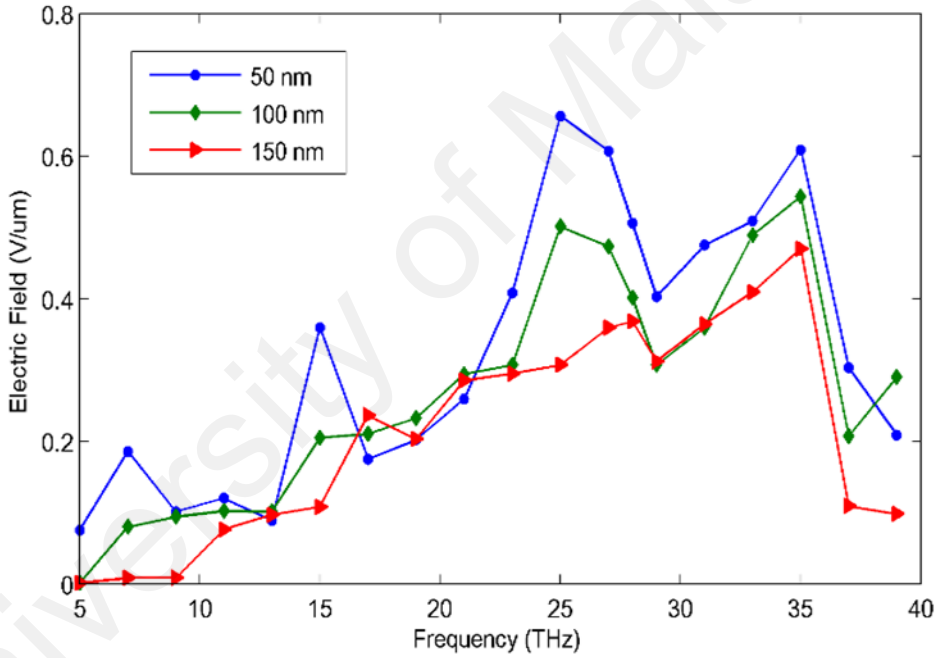

Figure 4.3: Variation of electric field versus frequency for different gap size.

4.2 Effect of gap size at the feeding point

Several numerical electromagnetic analyses are performed in order to optimize and find out the best fitted gap size at the feeding point of the antenna. After capturing the maximum electric field at the gap of the antenna, it transfers through the feeding line. In this investigation, it is concluded that, gap size can play an important role on the captured electric field. As observed in Figure 4.3, the maximum value of the electric field is found

in lower gap size (i.e., at 50 nm) provided that electric field tends to go low with lowering the gap.

4.3 Effect of feeding line thickness

In this subsection, the effect of feeding line thickness has been thoroughly studied. The dimension of antenna structure has been changed by varying the thickness of the feeding line. Figure 4.1 shows that the simulated return loss variation as a function of frequency for different feeding line thickness. As seen in the graph, there is slightly variation of the return loss and the best fitted thickness is 110 nm. But the electric field intensity is large at the lower thickness of the feeding line.

Figure 4.4 shows the variation of the voltage standing wave ration (VSWR) with the change of feeding line thickness. From the Figure 4.1 and Figure 4.3, it can be concluded that the best fitted curve for the energy harvesting purpose between the frequency range of 23.2 THz to 27 THz (bandwidth of 3.8 THz) and from 31 THz to 35.9 THz (bandwidth of 4.9 THz) has the feeding line thickness of 110 nm.

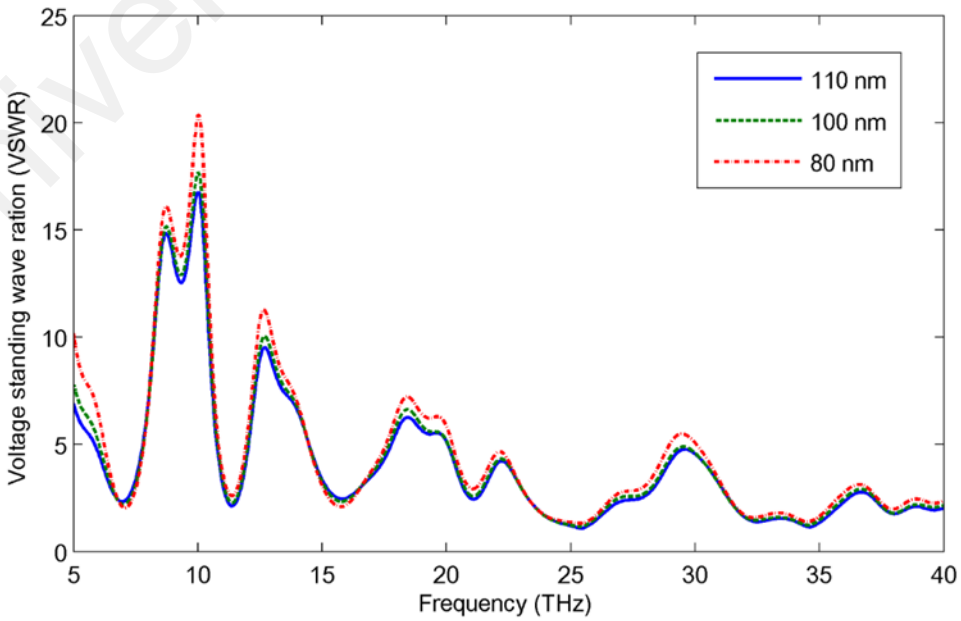

Figure 4.4: Variation of voltage standing wave ration versus frequency for different thickness of feed line.

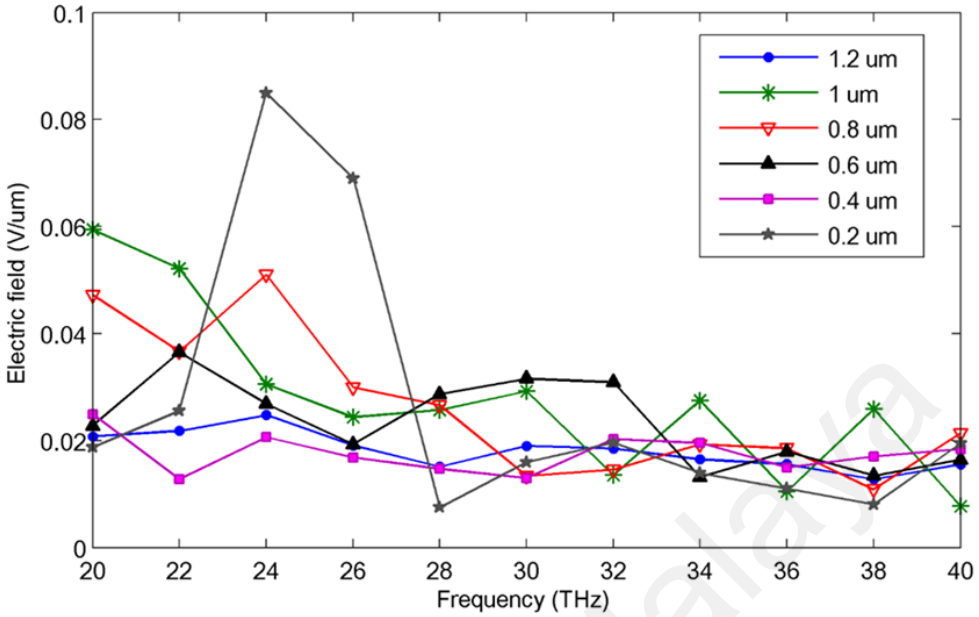

Figure 4.5: Variation of the electric field versus frequency for different substrate thickness of the circular edges bow-tie nano-antenna.

4.4 Effect of substrate thickness

The effect of substrate thickness on the electric field intensity, return loss, current density and voltage standing wave ratio of the circular edges bow-tie nano-antenna has been discussed here. The numerical electromagnetic analysis of the antenna has been performed by changing the thickness of the substrate. From the Figure 4.5, it is clear that the lower the substrate thickness, the higher the electric field intensity. Figure 4.6 depicts that the operating bandwidth of the antenna has changed with the variation of the substrate thickness. Current density has also been changed with the changing of the substrate thickness. It can also be observed that from Figure 4.3, Figure 4.7 and Figure 4.6 the maximum current density has been found at 1.2 μm substrate thickness.

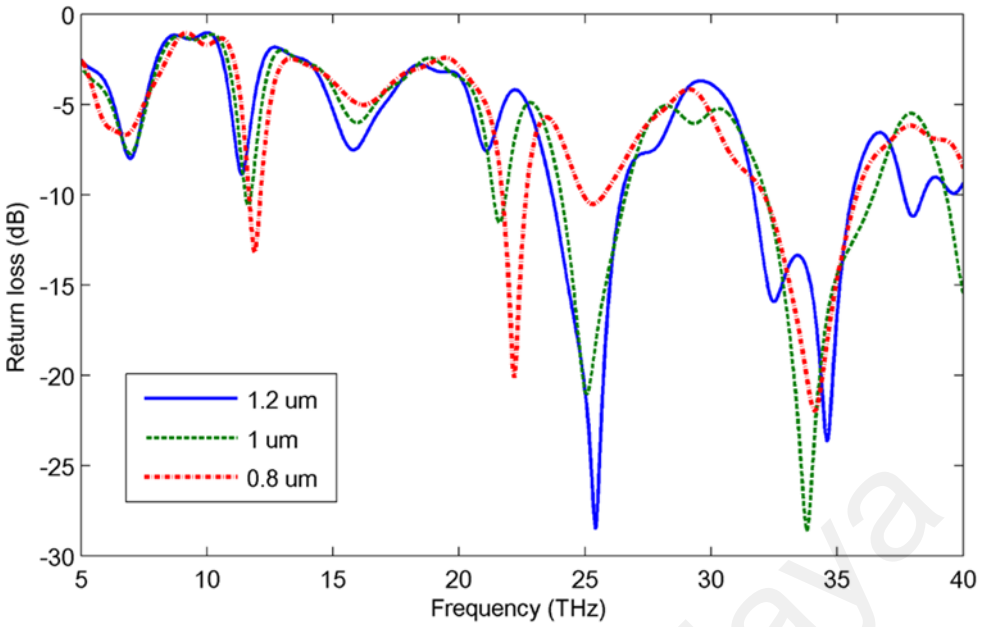

Figure 4.6: Variation of return loss versus frequency for different thickness of substrate.

Finally, performance comparison between the conventional spiral antenna and proposed circular edge bow-tie nano-antenna on the basis of their corresponding first and second bandwidth, frequency range, gain, geometric structure and impedance bandwidth is reported in Table 4.1. It is found that the proposed circular edge bow-tie nano-antenna offers wider bandwidth with multiple resonance frequency.

However, to convert the electric field into electricity, a suitable MIM (metal insulator metal) diode can be implanted for rectifying the received signal in the feeding gap. Using electron-beam lithography (EBL) (Biagioni et al., 2012; Ghenuche, Cherukulappurath, Taminiau, van Hulst, & Quidant, 2008; A Kumar, Hsu, Jacobs, Ferreira, & Fang, 2011; Anil Kumar et al., 2008; Muskens, Giannini, Sanchez-Gil, & Gómez Rivas, 2007; Schnell et al., 2009; Schuck, Fromm, Sundaramurthy, Kino, & Moerner, 2005) technique the designed antenna can be fabricated. EBL is one of the most popular techniques also to fabricate nano-antenna by using a flat substrate. In the typical process of EBL, a focused electron beam is employed for patterning high resolution electron sensitive resist, e.g.,

poly methyl methacrylate (PMMA). Afterwards, the pattern is selectively removed when it is developed. To cover both the voids and remaining resist, a thin layer of metal with desired thickness is then evaporated. Finally, a solvent is used on the sample to further remove the remaining resist so that the metal structure in the voids can be taken as unaffected.

Table 4.1: Performance comparison of the proposed circular edge bow-tie nano-antenna with conventional spiral antenna.

Topic	**Conventional Spiral Antenna (Gallo et al., 2012)**	**Proposed Circular Edge Bow-Tie Nano-antenna**
First bandwidth	(20 to 24.8 THz) 4.8 THz	(23.2 to 27 THz) 3.8 THz
Second bandwidth	(28 to 29.1 THz) 1.1 THz	(31 to 35.9 THz) 4.9 THz
Frequency swept	20 to 40 THz	5 to 40 THz
Directivity	8.61 dBi	8.57 dBi
Structure	Complicated spiral	Simple bow-tie
Microstrip line	Width=0.45 μm and length =29 μm	Width=50 nm and length = 9 μm
Impedance bandwidth	4.8 THz (21.5%) and 1.1 THz (3.88%)	3.8 THz (15.14%) and 4.9 THz (14.65%)

During the rectification process by MIM diode, re-radiation of higher harmonics is generated by this nonlinear diode and is responsible for some power loss. A low pass filter may be fixed in the middle of the antenna and MIM diode in order to eradicate this problem. This filter can also develop the impedance matching between the antenna and subsequent circuit. The analysis also provides a need of optimization of the geometrical structure and the antenna parameters, i.e., substrate thickness, feeding line width and the gap at the feeding point, in order to operate the designed antenna efficiently. It is recommended that the antenna should be an ad-hoc design in order to activate a wider

frequency band as the wave length are changed with the heat radiation and thermal radiation intensity. Antenna design with this technology can also be used to remove heat and serves as a cooling system in the electronic devices, etc. (Gallo et al., 2012). The Table 4.2 depicts simulation results for impedance bandwidth corresponds to the maximum return loss values.

Table 4.2: Impedance Bandwidth and Return loss (Simulation result)

At -10 dB f_l and f_h Frequency (THz)	Impedance Bandwidth (THz)	Return Loss (dB)
23.2 and 27	3.8 (15.14%)	-29.20
31 and 35.9	4.9 (14.65%)	-24.50

4.5 Surface current, current density and VSWR

For a good performing antenna, it is essential to have Voltage Standing Wave Ratio (VSWR) below the value of 2 at the operating frequencies used in different applications. From the Figure 4.7, it is clearly observed that VSWR is below 2 for the two operating range of frequencies from 23.2 THz to 27 THz (Bandwidth 3.8 THz) and from 31 THz to 35.9 THz (Bandwidth 4.9 THz) from the simulation results.

Figure 4.7 shows the direction of current from the antenna surface towards the feeding point. The surface current that is flowing through the designed antenna at the terahertz frequency band got from the CST Microwave Studio is shown in Figure 4.7 As observed; the maximum current intensity is obtained at the feeding point of the antennas. It can be clearly observed from the following figures that, surface current flowing through the designed antenna at the terahertz frequency are low and quite similar, which is desired for well performed antenna. A micro strip line has been used in order to collect the induced field from that gap.

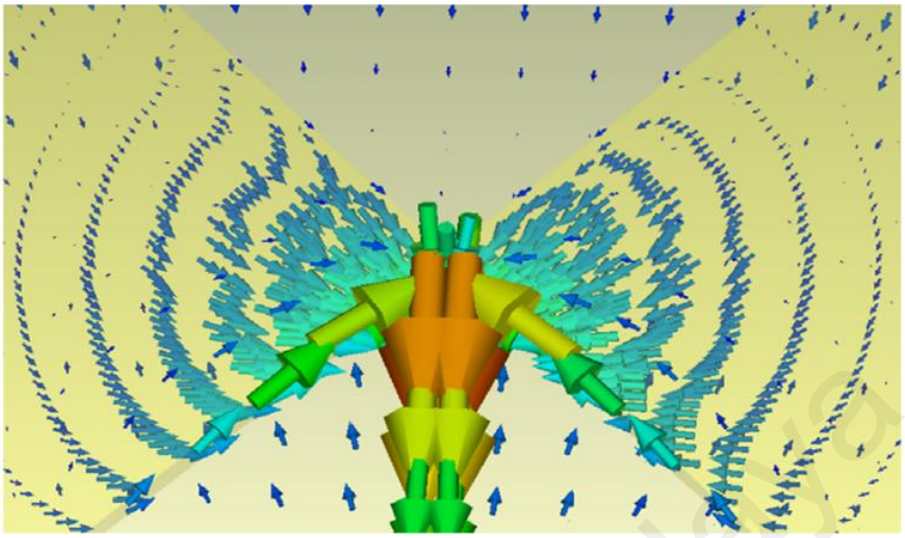

(b)

Figure 4.7: Direction of current flow of the nano-antenna concentrated at the feed point.

4.6 Slotting effect of circular edge bow-tie nano-antenna

In this section, the slotting effect in case of the design of a circular-shaped bowtie nano-antenna is demonstrated, which are different from the commercial solar panels used for energy harvesting .The optimum characterization of the designed nano-antenna has been analysed with respect to the number of slots using 3D electromagnetic solver. The electric field (V/μm) and the captured radiation bandwidth are the key parameters to figure out the performance of the conceptual antenna. The antenna consists of bow-tie triangular shape with circular edges made of gold thin film printed on a SiO_2 substrate placed on a ground plane at the back. The detailed geometric structure is depicted in Figure 4.8 of the circular edges bow-tie antenna with double slot.

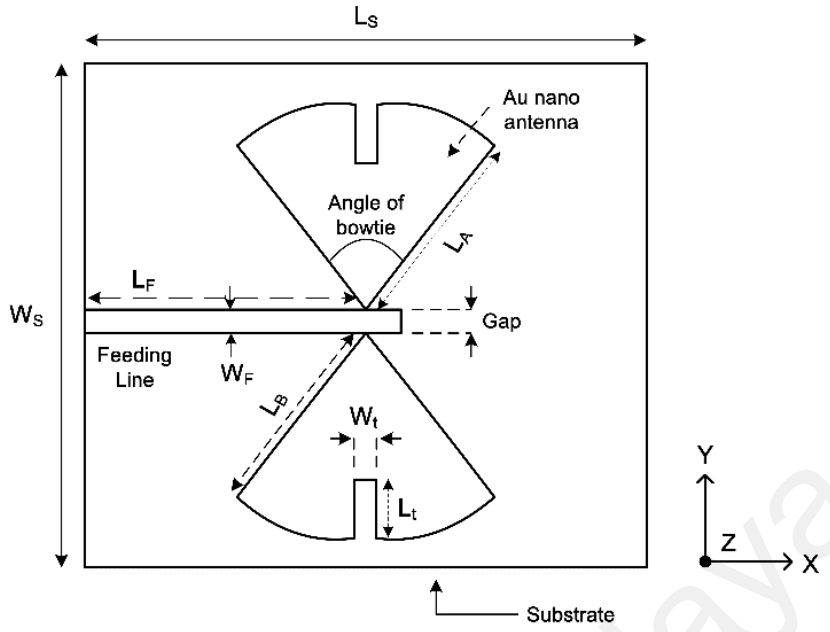

Figure 4.8: Details of the circular edges bow-tie antenna with double slot.

In this work, a circular edge bow-tie antenna comprise of triangular shape, having a suitable gap between their tips is proposed. The proposed structure is printed on a substrate of 18 ×18 μm^2. The permittivity of the substrate and thickness is considered to be 4.86 and 1.2 μm, respectively. A gold film of 150 nm thickness is selected to create the ground plane and antenna arms. The numerical investigation has achieved with a 3D electromagnetic solver. The proposed antenna is designed to receive induced electric field at the central gap. The electric field is then transferred via a feeding line and converted into electric current to supply the load. Figure 4.9 demonstrates the three dimensional geometric structure of the antenna of Figure 4.8. The yellow trace indicates the gold nano-antenna and the feeding line. The bright gray indicates the substrate of the antenna.

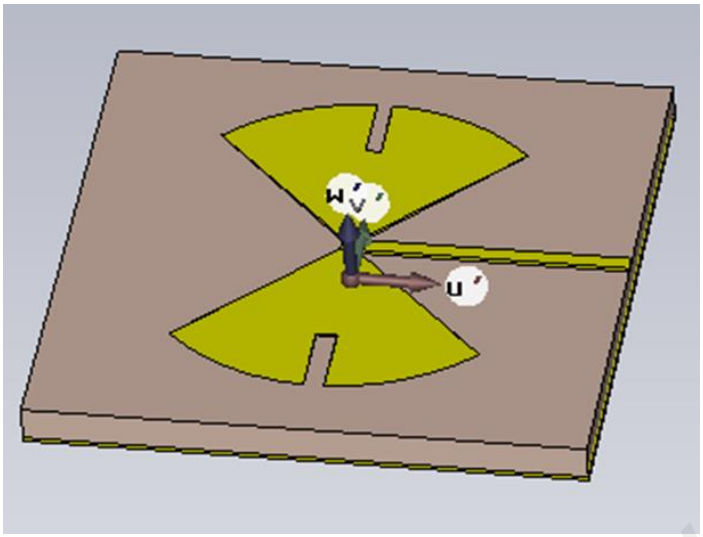

Figure 4.9: Three dimensional geometric structure of circular edge bow-tie nano-antenna with dual slot.

Now, slotting effect in designing the circular edge bow-tie nano-antenna with a rectangular air gap has been considered. The conceptual structure is gold printed on the 18×18 μm^2 substrate having 4.86 of permittivity, and 1.2 µm of thickness. The antenna and the ground plane consist of gold materials having thickness 150 nm. Figure 4.9 shows the three dimensional geometric structure of the designed nano-antenna. The length of the feeding line is considered as 9 µm and width of 110 nm.

Figure 4.10 shows the simulated return loss of the proposed antenna versus the frequency with the variation of the slot number in order to analyse the performance of the antenna. As seen, this antenna provides better performance around the frequency of 28.3 THz, which also shows multiple resonance frequencies. It exhibits return loss values below RL = -10 dB from 14 THz to 16 THz (bandwidth 2 THz), 19 THz to 24 THz (bandwidth 5 THz), 25 THz to 30 THz (bandwidth 5 THz) and 34 THz to 40 THz (6 THz), respectively.

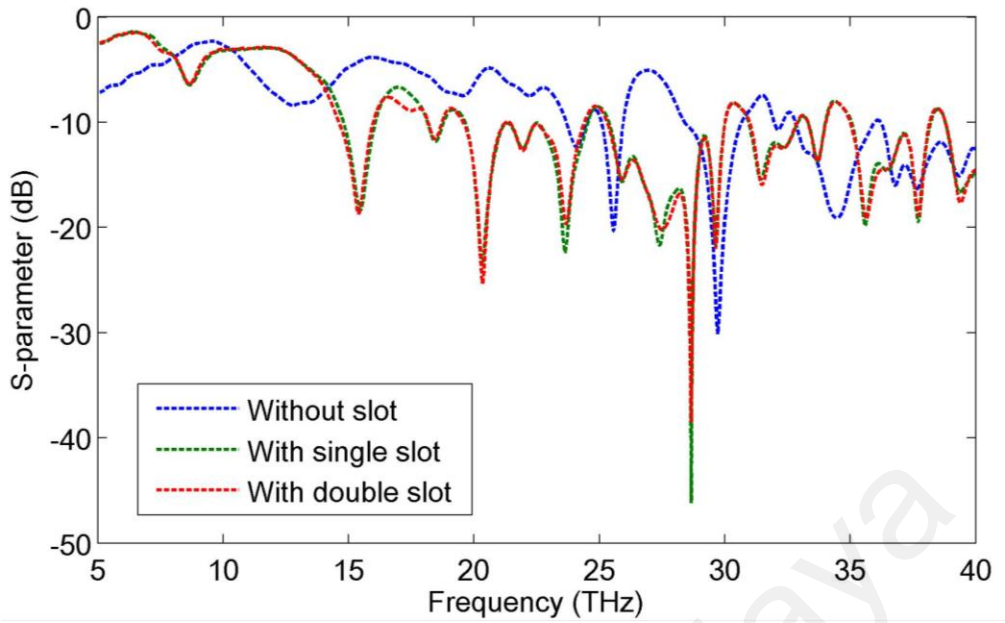

Figure 4.10: Variation of return loss versus frequency for different slotting.

In order to enhance the effectiveness of the antenna, this slotting feature could be used as earth radiated sun's energy in a broader frequency range. From the analysis, it is also clear that the antenna with double slot provides better electric field as well as wider bandwidth. The double slot antenna is more preferable because it also reduces antenna material as well. The gained numerical outcomes indicate the radiation pattern has a supreme directivity of 7.76 dBi. The half-power beam width is an important factor for the receiving of thermal radiation from diverse direction and hence this antenna is capable of capturing energy from the different directions. Figure 4.11 shows the 3D radiation pattern of the simulated antenna showing the directivity.

With the purpose of evaluating the electric field at the canter of the bow-tie tip in collecting solar energy and thermal energy, several simulations have been done by enlightening the antenna with a circularly polarized plane wave. Figure 4.12 depicts the calculated electric field versus frequencies for different slots.

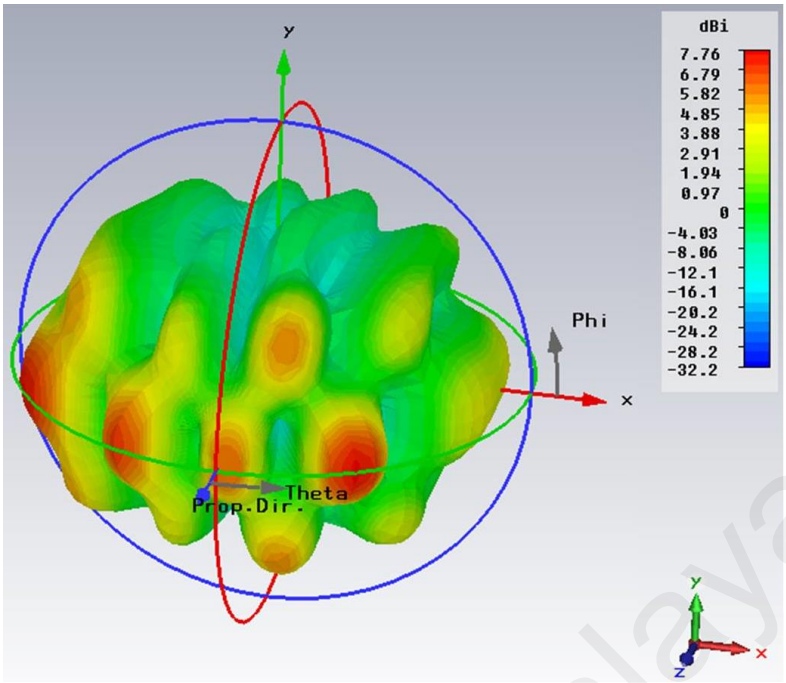

Figure 4.11: 3D radiation pattern of the simulated antenna.

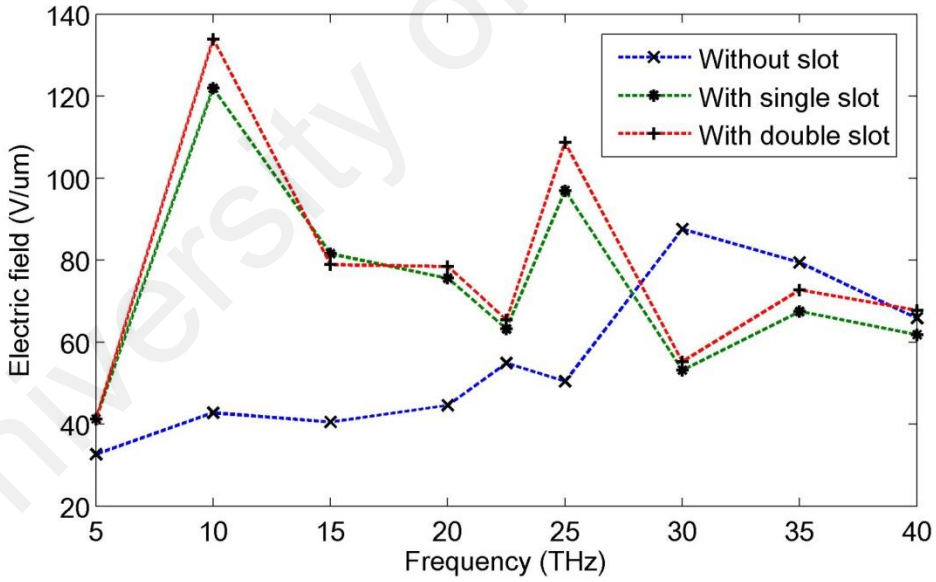

Figure 4.12: Variation of electric field versus frequency for different slotting.

As observed, the nano-antenna with double slot provides better electric field compared to that having single slot and without slot, respectively. A number of simulations are

performed in order to find out the best fitted return loss, electric field intensity and bandwidth limit.

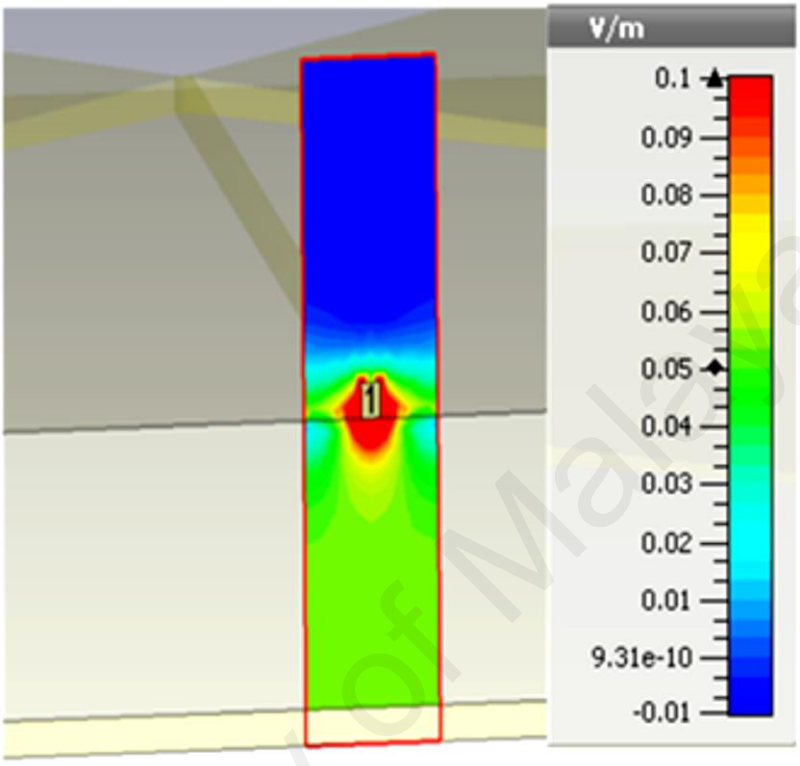

Figure 4.13: Electric field at the end of the feeding line.

A frequency sweep from 5 THz to 40 THz has been used to investigate the electromagnetic analysis. The electric field magnitude at the bow-tie tip and the wider bandwidth with better return loss are the key parameters to measure the performance of the bow-tie nano-antenna. Figure 4.13 represents the electric field at the feeding line end of the antenna. From the numerical electromagnetic simulation, it is observed that, the feed point of the antenna is the best location to harvest the solar and earth thermal energy as this point provides maximum electric field. Specially, the free electron of the gold material movement towards the antenna's surface and intensifies at the antenna feed point. The harvested electric field is not sufficient due to the technological limitations. Number of slots has a significant effect on both electric field and antenna bandwidth

where antenna with double slot provides better electric field and wider bandwidth as compared to the antenna without slot. Figure 4.14 shows the 2D radiation pattern of the simulated antenna at 28.3 THz without slot, and with single and double slots. Considering overall performance including electric filed, antenna materials and return loss antenna with double slot perform well.

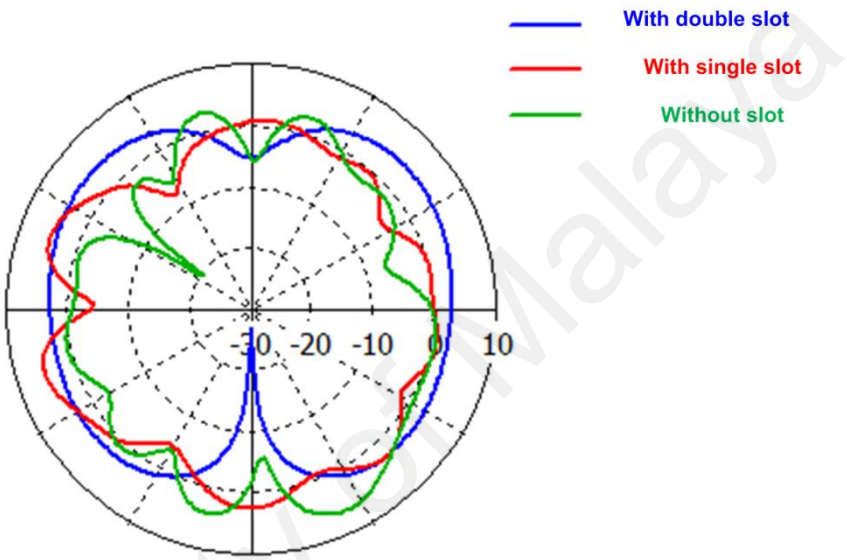

Figure 4.14: 2D radiation pattern of the simulated antenna at 28.3 THz.

4.7 Parametric Analyses

Parametric analyses are done with the help of the CST Microwave Studio in order to inspect the effects of different key design parameters on the impedance bandwidth of the proposed nano-antenna with a ground plane. These analyses have been accomplished by changing one design parameter whilst other parameters are had unchanged to observe the real change of the performance for the specific parameter. The preferred key design parameters of this antenna are the thickness of the substrate, gap between the bow-tie tip and width of the feeding line etc. Here, investigation of return loss as well as impedance bandwidth are being observed by the variation of selected important parameters that have significant impact on the factors of performance. In

Figure **4.15** variation of electric field (V/um) at different gap size between the bow-tie tip are presented. It is clearly seen from the figure that maximum electric field has achieved at the 50 nm gap size between the bow-tie tip. In Figure 4.16 return losses at different feeding line thickness are presented. It is clearly seen from the figure that impedance bandwidth and return loss changes with the thickness of the feeding line and broadest bandwidth has achieved at the 110 nm feeding line thickness.

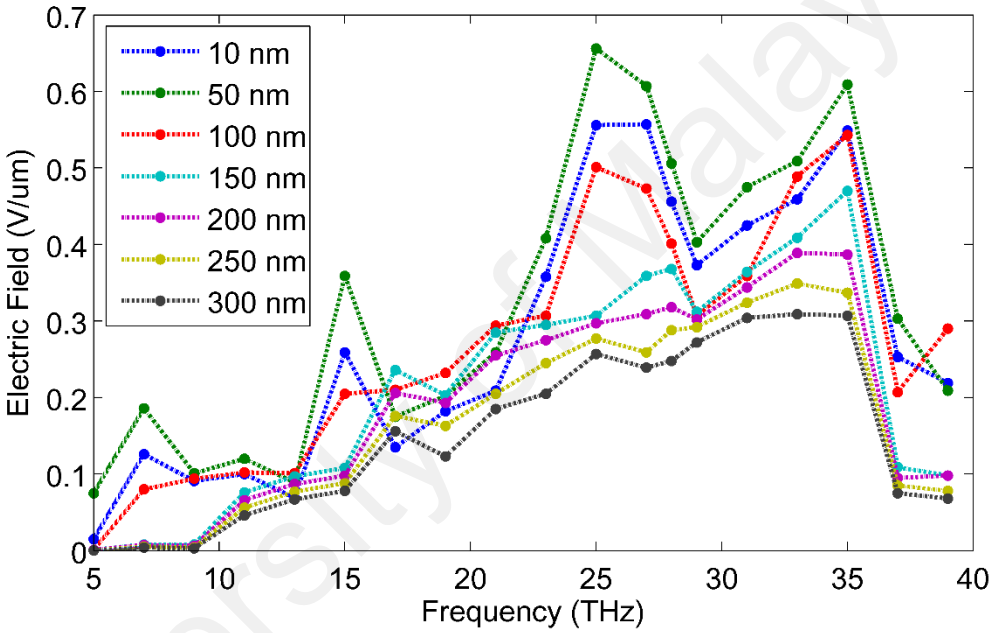

Figure 4.15: Simulated electric field (V/um) vs frequency (THz) at different gap size between the bow-tie tip.

Effects of the variation of the width of substrate thickness on the impedance bandwidth are represented in the Figure 4.17. Ground plane is being used for this antenna having width of 150 nm. It is witnessed from the above figure that return loss and impedance bandwidth are considerably decreased with the enhancement of the width of substrate and feeding line and good results are obtained for the width dimension of 1.2 µm and 110 nm respectively.

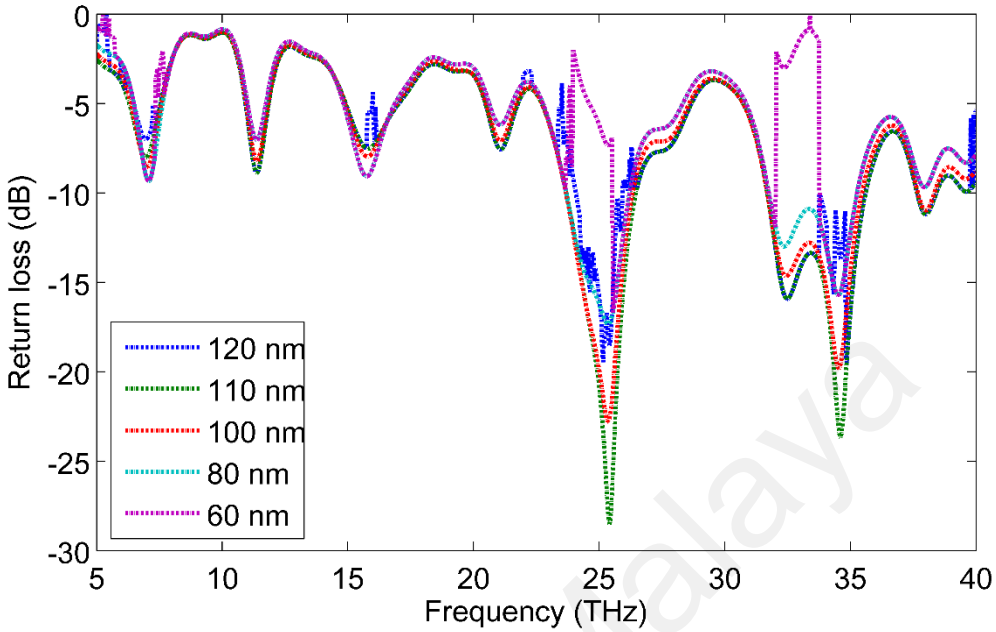

Figure 4.16: Simulated return losses at different width of feeding line.

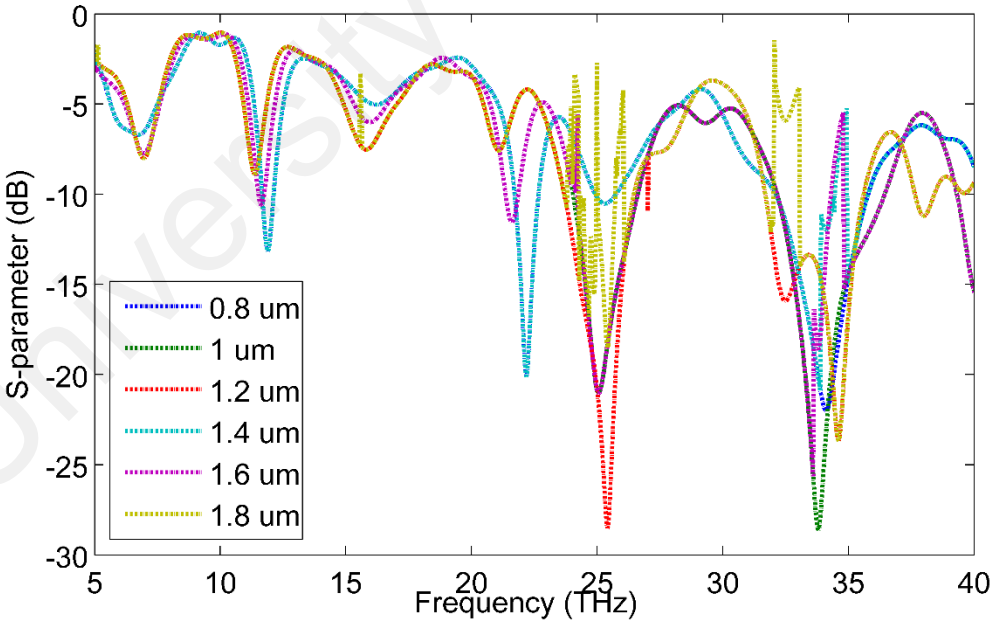

Figure 4.17: Simulated return losses at different substrate thickness.

Return loss and impedance bandwidth decrease with the increment of the width of substrate thickness and feeding line when it is 1.2 µm and 110 nm respectively. The

greatest bandwidth obtained at the width of 1.2 µm substrate thickness and 110 nm feeding line width.

4.8 Summary

In this chapter, several performance parameter evaluations are presented and the results are critically analysed. The effect of return loss, impedance bandwidth, surface current, voltage standing wave ratio (VSWR), current density, radiation pattern, and gain have been investigated in details. The designed antenna has shown a better performance around the frequency 25.3 THz with a feeding line thickness of 110 nm. This antenna provides multiple resonance frequency. It is observed that, the return loss value stays below -10 dB from 23.2 THz to 27 THz (Bandwidth 3.8 THz) and from 31 THz to 35.9 THz (Bandwidth 4.9 THz). This feature helps to capture the radiation in a wider frequency range in order to harvest energy from the earth radiated and infrared band. It also provides a better directivity with a maximum value of 8.57 dBi. An output electric field of 0.656 V/µm is simulated at 25.3 THz. The best fitted gap size at the feed point is achieved as 50 nm with the substrate thickness of 1.2 µm. Slotting effect in return loss, resonance frequency, electric field (V/µm) and directivity for the designed antenna has also been discussed and analysed in details.

CHAPTER 5: CONCLUSION

5.1 Overall conclusion

In this work, an investigation of circular edges bow-tie nano-antenna for far-infrared band has been presented which is capable of collecting the radiation emitted from the earth and harvesting solar energy to transfer them into electricity. The electromagnetic analysis of the designed nano-antenna has been performed through simulation by adding a microstrip line fixed to the substrate. A circularly polarized plane wave has been used in order to illuminate the antenna due to the analysis of radiation characteristics. Lorentz-Drude model has been considered during the analysis of dispersive characteristic of gold material at the terahertz frequency band. The designed circular shaped bowtie nano-antenna exhibits resonant frequency at 25.3 THz and shows a better return loss value within the frequency band of 23.2 THz to 27 THz (bandwidth 3.8 THz) and from 31 THz to 35.9 THz (bandwidth 4.9 THz). This antenna provides maximum electric field intensity at 25.3 THz with a substrate thickness of 1.2 μm and with an inter bow-tie tip gap of 50 nm. This novel antenna shows multiple resonances which is useful in the field of energy harvesting application. At the first resonant the maximum electric field of 0.359 V/μm has been obtained at 15 THz, where at the second resonant maximum electric field of 0.656 V/μm has been achieved at 25.3 THz and at the third resonant this field has been obtained at 35 THz with 0.609 V/μm. In this study, a brief investigation has been performed on the effect on the electric field intensity with the variations of substrate thickness, feeding line width, no of slots and the gap at the feeding point between bow-tie tips. From the results, it is observed that the effects of these parameters have clear impacts on the electric field and the resonance frequency. If technological limitation in the field of fabrication is overcome, then the nanorectenna will be capable of efficiently collect the energy at the infrared wavelengths and will replace the traditional solar cells.

The nano-antenna is also able to operate at night, which can overcome the main drawback of conventional solar system.

5.2 Future works

For the next generation of application, nano-antennas are holding enough promises. In view of currently achieved investigation results and the state-of-art nano-antenna research swings, extensive further research can be foreseen easily. In this work, a theoretical study on the nano-antenna consisting gold material on the SiO_2 substrate is presented, focusing on their favourable optical properties for the application of energy harvesting from infrared and THz frequency region. There are some limitations in the presented design which require improvement and further extension. Firstly, the source utilized in the presented research is a single type plane wave excitation. Other kinds of light sources can be applied to illuminate nano-antenna in order to develop a systematically study. Secondly, this work is limited to simple geometrical structure like, length of the antenna, the width of the feed line, thickness of the substrate and the gap between the antennas which are investigated in details. Other dimensions can be investigated in the same way also which holds for the further research scopes. Basic principles and reliability assessment should be considered throughout the transformation. In order to operate the antenna for the optical application, there are some requirements to explore more kinds of nano-antennas in the near future. Further research activities may be foreseen to identify the effectiveness of the integrated array of nano-antennas with MIM diode also.

REFERENCES

Atwater, H. A., & Polman, A. (2010). Plasmonics for improved photovoltaic devices. *Nature materials, 9*(3), 205-213.

Bachelot, R., Gleyzes, P., & Boccara, A. (1995). Near-field optical microscope based on local perturbation of a diffraction spot. *Optics letters, 20*(18), 1924-1926.

Balanis, C. A. (2012). *Antenna theory: analysis and design*: John Wiley & Sons.

Bareiss, M., Hochmeister, A., Jegert, G., Koblmuller, G., Zschieschang, U., Klauk, H., Lugli, P. (2011). Energy harvesting using nano-antenna array. Paper presented at the *Nanotechnology (IEEE-NANO), 2011 11th IEEE Conference on*.

Bean, J. A., Tiwari, B., Bernstein, G. H., Fay, P., & Porod, W. (2009). Thermal infrared detection using dipole antenna-coupled metal-oxide-metal diodes. *Journal of Vacuum Science & Technology B, 27*(1), 11-14.

Bean, J. A., Weeks, A., & Boreman, G. D. (2011). Performance optimization of antenna-coupled tunnel diode infrared detectors. *Quantum Electronics, IEEE Journal of, 47*(1), 126-135.

Berland, B. (2003). Photovoltaic technologies beyond the horizon: optical rectenna solar cell: NREL/SR-520-33263.

Bharadwaj, P., Deutsch, B., & Novotny, L. (2009). Optical antennas. *Advances in Optics and Photonics, 1*(3), 438-483.

Bhunia, S. (2012). Effects of Slot Loading on Microstrip Patch Antennas. *International Journal of Wired and Wireless Communications, 1*(1), 1-6.

Biagioni, P., Huang, J.-S., & Hecht, B. (2012). Nano-antennas for visible and infrared radiation. *Reports on Progress in Physics, 75*(2), 024402.

Bozzetti, M., de Candia, G., Gallo, M., Losito, O., Mescia, L., & Prudenzano, F. (2010). Analysis and design of a solar rectenna. Paper presented at the *Industrial Electronics (ISIE), 2010 IEEE International Symposium on.*

Briones, E., Alda, J., & González, F. J. (2013). Conversion efficiency of broad-band rectennas for solar energy harvesting applications. *Optics express, 21*(103), A412-A418.

Briones, E., Briones, J., Cuadrado, A., Martinez-Anton, J. C., McMurtry, S., Hehn, M., . . . Gonzalez, F. J. (2014). Seebeck nano-antennas for solar energy harvesting. *Applied Physics Letters, 105*(9), 093108.

Briones, E., Briones, J., Cuadrado, A., Murtry, S. M., Hehn, M., Montaigne, F., . . . González, F. J. (2014). Computational Analysis of a Spiral Thermoelectric Nano-antenna for Solar Energy Harvesting Applications. *arXiv preprint arXiv:1401.4971*.

Brown, W. C. (1976). Optimization of the efficiency and other properties of the rectenna element. Paper presented at the *Microwave Symposium, 1976 IEEE-MTT-S International.*

Catchpole, K., & Polman, A. (2008). Plasmonic solar cells. *Optics express, 16*(26), 21793-21800.

Chen, Z., Li, X., Taflove, A., & Backman, V. (2006). Backscattering enhancement of light by nanoparticles positioned in localized optical intensity peaks. *Applied optics, 45*(4), 633-638.

Corkish, R., Green, M., & Puzzer, T. (2002). Solar energy collection by antennas. *Solar Energy, 73*(6), 395-401.

Derkacs, D., Chen, W., Matheu, P., Lim, S., Yu, P., & Yu, E. (2008). Nanoparticle-induced light scattering for improved performance of quantum-well solar cells. *Applied Physics Letters, 93*(9), 091107.

Dmitruk, N., Malynych, S., Moroz, I., & Kurlyak, V. Y. (2010). Optical efficiency of Ag and Au nanoparticles. *Semiconductor Physics, Quantum Electronics & Optoelectronics, 13*(4), 369-373.

Feichtner, T., Selig, O., Kiunke, M., & Hecht, B. (2012). Evolutionary optimization of optical antennas. *Physical Review Letters, 109*(12), 127701.

Fumeaux, C., Herrmann, W., Kneubühl, F., & Rothuizen, H. (1998). Nanometer thin-film Ni–NiO–Ni diodes for detection and mixing of 30 THz radiation. *Infrared Physics & Technology, 39*(3), 123-183.

Fumeaux, C., Herrmann, W., Rothuizen, H., De Natale, P., & Kneubühl, F. (1996). Mixing of 30 THz laser radiation with nanometer thin-film Ni-NiO-Ni diodes and integrated bow-tie antennas. *Applied Physics B, 63*(2), 135-140.

Gadalla, M., Abdel-Rahman, M., & Shamim, A. (2014). Design, Optimization and Fabrication of a 28.3 THz Nano-Rectenna for Infrared Detection and Rectification. *Scientific reports, 4*.

Gallo, M., Mescia, L., Losito, O., Bozzetti, M., & Prudenzano, F. (2012). Design of optical antenna for solar energy collection. *Energy, 39*(1), 27-32.

Genov, D. A., Sarychev, A. K., Shalaev, V. M., & Wei, A. (2004). Resonant field enhancements from metal nanoparticle arrays. *Nano Letters, 4*(1), 153-158.

Ghenuche, P., Cherukulappurath, S., Taminiau, T. H., van Hulst, N. F., & Quidant, R. (2008). Spectroscopic mode mapping of resonant plasmon nano-antennas. *Physical Review Letters, 101*(11), 116805.

Gotschy, W., Vonmetz, K., Leitner, A., & Aussenegg, F. (1996). Optical dichroism of lithographically designed silver nanoparticle films. *Optics letters, 21*(15), 1099-1101.

Grober, R. D., Schoelkopf, R. J., & Prober, D. E. (1997). Optical antenna: Towards a unity efficiency near-field optical probe. *Applied Physics Letters, 70*(11), 1354-1356.

Heikkinen, J., & Kivikoski, M. (2003). A novel dual-frequency circularly polarized rectenna. *Antennas and Wireless Propagation Letters, IEEE, 2*(1), 330-333.

Huang, J.-S., Feichtner, T., Biagioni, P., & Hecht, B. (2009). Impedance matching and emission properties of nano-antennas in an optical nanocircuit. *Nano Letters, 9*(5), 1897-1902.

Hussein, M., Areed, N. F. F., Hameed, M. F. O., & Obayya, S. S. A. (2014). Design of flower-shaped dipole nano-antenna for energy harvesting.*IET Optoelectronics*, 8(4), 167-173

Kattawar, G., Li, C., Zhai, P.-W., & Yang, P. (2005). Electric and magnetic energy density distributions inside and outside dielectric particles illuminated by a plane electromagnetic wave. *Optics express, 13*(12), 4554-4559.

Kocakarin, I., & Yegin, K. (2013). Glass superstrate nano-antennas for infrared energy harvesting applications. *International Journal of Antennas and Propagation, 2013*.

Kotter, D. K., Novack, S. D., Slafer, W. D., & Pinhero, P. (2008). Solar nantenna electromagnetic collectors. Paper presented at the *ASME 2008 2nd International*

Conference on Energy Sustainability collocated with the Heat Transfer, Fluids Engineering, and 3rd Energy Nanotechnology Conferences.

Kottmann, J., Martin, O., Smith, D., & Schultz, S. (2000). Spectral response of plasmon resonant nanoparticles with a non-regular shape. *Optics express, 6*(11), 213-219.

Krishnan, S., La Rosa, H., Stefanakos, E., Bhansali, S., & Buckle, K. (2008). Design and development of batch fabricatable metal–insulator–metal diode and microstrip slot antenna as rectenna elements. *Sensors and Actuators A: Physical, 142*(1), 40-47.

Kumar, A., Hsu, K., Jacobs, K., Ferreira, P., & Fang, N. (2011). Direct metal nano-imprinting using an embossed solid electrolyte stamp. *Nanotechnology, 22*(15), 155302.

Kumar, A., Hsu, K. H., Chaturvedi, P., Ma, H., Xu, J., & Fang, N. X. (2008). Fabrication and optical characterization of bowtie antennas. Paper presented at the *Nanotechnology*, 2008. NANO'08. 8th IEEE Conference on.

Ma, Z., & Vandenbosch, G. A. (2013a). Optimal solar energy harvesting efficiency of nano-rectenna systems. *Solar Energy, 88*, 163-174.

Ma, Z., & Vandenbosch, G. A. (2013b). Systematic Full-Wave Characterization of Real-Metal Nano Dipole Antennas.

Ma, Z., Zheng, X., Vandenbosch, G. A., & Moshchalkov, V. (2013). *On the efficiency of solar energy harvesting with nano-dipoles.* Paper presented at the Antennas and Propagation (EuCAP), 2013 7th European Conference on.

Makarov, S. (2002). *Antenna and EM Modeling with MATLAB* (Vol. 1): Princeton University Press.

Maksymov, I. S., Staude, I., Miroshnichenko, A. E., & Kivshar, Y. S. (2012). Optical yagi-uda nano-antennas. *Nanophotonics, 1*(1), 65-81.

McMahon, J. M., Gray, S. K., & Schatz, G. C. (2010). Optical properties of nanowire dimers with a spatially nonlocal dielectric function. *Nano Letters, 10*(9), 3473-3481.

McSpadden, J. O., Yoo, T., & Chang, K. (1992). Theoretical and experimental investigation of a rectenna element for microwave power transmission. *Microwave Theory and Techniques, IEEE Transactions on, 40*(12), 2359-2366.

Muskens, O., Giannini, V., Sanchez-Gil, J., & Gómez Rivas, J. (2007). Strong enhancement of the radiative decay rate of emitters by single plasmonic nano-antennas. *Nano Letters, 7*(9), 2871-2875.

Nehl, C. L., Liao, H., & Hafner, J. H. (2006). Optical properties of star-shaped gold nanoparticles. *Nano Letters, 6*(4), 683-688.

Novotny, L. (2007). Effective wavelength scaling for optical antennas. *Physical Review Letters, 98*(26), 266802.

Park, J.-Y., Han, S.-M., & Itoh, T. (2004). A rectenna design with harmonic-rejecting circular-sector antenna. *Antennas and Wireless Propagation Letters, IEEE, 3*(1), 52-54.

Planck, M. (1910). Zur Theorie der Wärmestrahlung. *Annalen der Physik, 336*(4), 758-768.

Rakić, A. D., Djurišić, A. B., Elazar, J. M., & Majewski, M. L. (1998). Optical properties of metallic films for vertical-cavity optoelectronic devices. *Applied optics, 37*(22), 5271-5283.

Sabaawi, A. M., Tsimenidis, C. C., & Sharif, B. S. (2013). Planar Bowtie Nanoarray for THz Energy Detection. *IEEE Transaction on terahertz science and technology, 3(5),524-531*

Sánchez, E. J., Novotny, L., & Xie, X. S. (1999). Near-field fluorescence microscopy based on two-photon excitation with metal tips. *Physical Review Letters, 82*(20), 4014.

Schnell, M., Garcia-Etxarri, A., Huber, A., Crozier, K., Aizpurua, J., & Hillenbrand, R. (2009). Controlling the near-field oscillations of loaded plasmonic nano-antennas. *Nature Photonics, 3*(5), 287-291.

Schuck, P., Fromm, D., Sundaramurthy, A., Kino, G., & Moerner, W. (2005). Improving the mismatch between light and nanoscale objects with gold bowtie nano-antennas. *Physical Review Letters, 94*(1), 017402.

Shi, X., Hesselink, L., & Thornton, R. L. (2003). Ultrahigh light transmission through a C-shaped nanoaperture. *Optics letters, 28*(15), 1320-1322.

Slovick, B. A., Bean, J. A., Krenz, P. M., & Boreman, G. D. (2010). Directional control of infrared antenna-coupled tunnel diodes. *Optics express, 18*(20), 20960-20967.

Stockman, M., Faleev, S., & Bergman, D. (2002). Coherently controlled femtosecond energy localization on nanoscale. *Applied Physics B, 74*(1), s63-s67.

Stockman, M. I., Bergman, D. J., & Kobayashi, T. (2004). Coherent control of nanoscale localization of ultrafast optical excitation in nanosystems. *Physical Review B, 69*(5), 054202.

Studio, C. M. CST, Framingham, MA, USA, 2012.

Suh, Y.-H., & Chang, K. (2002). A high-efficiency dual-frequency rectenna for 2.45-and 5.8-GHz wireless power transmission. *Microwave Theory and Techniques, IEEE Transactions on, 50*(7), 1784-1789.

Sundaramurthy, A., Crozier, K., Kino, G., Fromm, D., Schuck, P., & Moerner, W. (2005). Field enhancement and gap-dependent resonance in a system of two opposing tip-to-tip Au nanotriangles. *Physical Review B, 72*(16), 165409.

Ulaby, F. T., Michielssen, E., & Ravaioli, U. (2010). *Fundamentals of applied electromagnetics*: Prentice Hall.

Vandenbosch, G. A., & Ma, Z. (2012). Upper bounds for the solar energy harvesting efficiency of nano-antennas. *Nano Energy, 1*(3), 494-502.

Wang, H., Brandl, D. W., Le, F., Nordlander, P., & Halas, N. J. (2006). Nanorice: a hybrid plasmonic nanostructure. *Nano Letters, 6*(4), 827-832.

Wang, J.-M., & Lu, C.-L. (2013). Design and Implementation of a Sun Tracker with a Dual-Axis Single Motor for an Optical Sensor-Based Photovoltaic System. *Sensors, 13*(3), 3157-3168.

Wilke, I., Oppliger, Y., Herrmann, W., & Kneubühl, F. (1994). Nanometer thin-film Ni-NiO-Ni diodes for 30 THz radiation. *Applied Physics A, 58*(4), 329-341.

Wu, Y.-M., Li, L.-W., & Liu, B. (2010). Gold bow-tie shaped aperture nano-antenna: Wide band near-field resonance and far-field radiation. *Magnetics, IEEE Transactions on, 46*(6), 1918-1921.

Yang, Y., Yeo, J., & Priya, S. (2012). Harvesting energy from the counterbalancing (weaving) movement in bicycle riding. *Sensors, 12*(8), 10248-10258.

Yu, H., Yue, Q., Zhou, J., & Wang, W. (2014). A Hybrid Indoor Ambient Light and Vibration Energy Harvester for Wireless Sensor Nodes. *Sensors*, *14*(5), 8740-8755.

LIST OF PUBLICATIONS

ISI-Cited Journal Papers:

1. **Haque, Ahasanul,** Ahmed Wasif Reza, and Narendra Kumar. "A Novel Design of Circular Edge Bow-Tie Nano Antenna for Energy Harvesting." Frequenz 69.11-12 (2015): 491-499.

Conferences:

1. **Ahasanul Haque**, Ahmed Wasif Reza, Narendra Kumar and Harikrishnan Ramiah, "Slotting effect in designing circular edge bow-tie nano-antenna for energy harvesting system," 2015 IEEE Conference on Open Systems (sponsored by IEEE Computer Society Malaysia), Malacca, Malaysia, 24-26 August 2015.